IN-RUSH CURRENT MITIGATION ON TOROIDAL TRANSFORMERS WITH SLOTTED CORE

Minura Gayan Karapitiya Pathirana

(168624K)

Degree of Master of Science

Department of Electrical Engineering

University of Moratuwa
Sri Lanka

April 2020

IN-RUSH CURRENT MITIGATION ON TOROIDAL TRANSFORMERS WITH SLOTTED CORE

Minura Gayan Karapitiya Pathirana

(168624K)

Dissertation submitted in partial fulfillment of the requirements for the degree of Master of Science in Electrical Installation

Department of Electrical Engineering

University of Moratuwa
Sri Lanka

April 2020

DECLARATION OF THE CANDIDATE AND SUPERVISORS

I declare that this is my own work and this dissertation does not incorporate without acknowledgment any material previously submitted for a Degree or Diploma in any other University or institute of higher learning and to the best of my knowledge and belief it does not contain any material previously published or written by another person except where the acknowledgement is made in the text.

Also, I hereby grant to University of Moratuwa the non-exclusive right to reproduce and distribute my dissertation, in whole or in part in print, electronic or other medium. I retain the right to use this content in whole or part in future works (such as articles or books).

………………………………

Signature of the candidate   Date

(M.G.K.Pathirana)

The above candidate has carried out research for the Masters dissertation under my supervision.

………………………………

Signature of the supervisor   Date

(Prof. J.P. Karunadasa)

// ACKNOWLEDGEMENT

First of all, I would like to express my sincere thanks to my supervisor, Professor J. P. Karunadasa, who gave me great support and guidance so that I can continue this research with motivation, enthusiasm and his extensive knowledge to be successful.

Furthermore, I would like to thank all the lecturers who participated in the Master’s degree program who broadened our horizons, and provided us with opportunities to improve knowledge in various fields.

Next, I would like to thank the company that I’m currently works at, Noratel International (Pvt) Ltd., which provides the research materials and facilities necessary to complete this research.

A sincere thanks to the prototyping department of the company for supporting me and giving me the support of sampling, which helped me a lot to collect the required data.

Also, I thank my friend Sameera for the help in my workplace and continued encouragement throughout the career.

Finally, I would like to thank my wife, mother, father and sister for their unwavering love and support in this difficult period.

M.G.K.Pathirana.

ABSTRACT

When it comes to transformer industry, toroidal transformers plays a major role, especially in high-tech applications, as they outperform traditional laminated transformers. However, toroidal transformers have a much higher inrush current, especially compared to laminate transformers, which will be a major drawback at the high power applications.

Currently there are many options available outside the toroidal transformer to avoid this inrush problem, but reliability issues will still there when using external inrush controlling mechanisms. Traditional inrush current mitigation methods on transformers are not sufficient for toroidal transformers. These methods tend to reduce good performance as well as inrush current.

The proposed inrush current mitigation method using a transformer-based slotted core, significantly reduces the inrush current while protecting the excellent performance characteristics which is typical for toroidal transformers. In addition, it offers better control of the inrush current than traditional methods.

The proposed method is a slotted core which has a slot in the outer periphery.
That controls the saturation inductance and hence the inrush current.
At the end, the slotted core maintains high performance without compromising normal operation.

This document includes a practical development of slotted cores and as well as experimental tests of inrush current, and finally a new design tool for the optimized deigns.

TABLE OF CONTENTS

LIST OF FIGURES

LIST OF TABLES

LIST OF ABBREVIATIONS

Abbreviation	**Description**
AC	Alternative Current
AISI	American Iron and Steel Institute
DC	Direct Current
EMI	Electro Magnetic Interference
GOSS	Grain Oriented Silicon Steel
H	Height
ID	Inner Diameter
IEC	International Electrotechnical Commission
MMF	Magneto Motive Force
MPL	Magnetic Path Length
NC	Nano Crystalline
NGOSS	Non Grain Oriented Silicon Steel
NTC	Negative Temperature Coefficient
OD	Outer Diameter
RMS	Root Mean Square

LIST OF APPENDICES

INTRODUCTION

Inrush current (sometimes called input surge current) is defined as maximum peak current drawn by electrical equipment due to driving its core into deep saturation at the time of energization. Inrush current is an undesirable phenomenon to occur and the equipment manufacturers/designers have to take this in to consideration where it is applicable. Elimination of inrush current could be very costly and impossible but mitigation of inrush current is possible [1].

Generally for all cases inrush current does not last for a long time. For example it lasts only for few cycles for alternating current (AC), for transformers and motors. Magnitude of inrush current to its rated current could be several times, or even closer to 30 times in extreme cases, especially with toroidal transformers [2]. The magnitude of the inrush current is based on several parameters like; switching angle, source impedance, magnitude of input voltage, residual flux on the core, saturation inductance, etc. As a result, more often overcurrent protection reacts for these high currents and trips the device from the source resulting inability to energize the equipment. Also the inrush current will result in significant voltage drops, and thus affect the power quality, reliability and stability [2].

Inrush current most of the time is harmless to the device but unwanted tripping could cause undue problems to the electrical system. But in special cases, mostly with toroidal transformers which normally connected at high end applications, it needs to protect the expensive power electronic equipment from the high currents [2].

To understand this phenomenon in transformers and motors it requires sound knowledge of mathematics and magnetism. Inrush current occurrences on transformers are explained in chapter 2 to the extent of the topic being discussed. Typical inrush current transient waveform when a transformer is energized is illustrated in Figure 1.1, which is captured on a single phase 1000VA toroidal transformer.

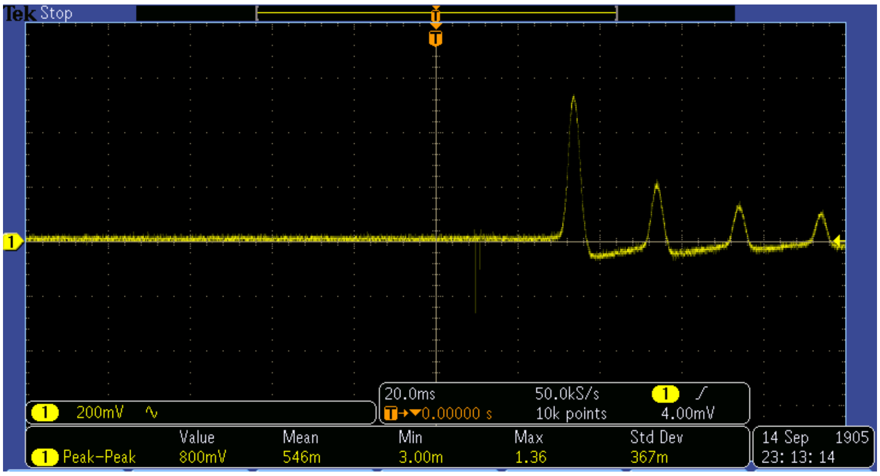

Figure 1.1: Inrush current transient waveform

1.1 Toroidal Transformer Construction

Toroidal winding is considered to be challenging with respect to winding in laminated transformer, as it required rotating the coil during winding through the inner diameter of the core. Typical toroidal core does not hold any gaps in its magnetic path, which cause the toroidal transformer to be high performing with respect to the laminated transformers. The performance of an ideal transformer can be closely approximated with this most expensive toroidal construction [1].

In the manufacturing process, sufficient winding wire must be loaded into the winding shuttle of the machine , and then wind onto the toroidal transformer's core as per the required turns in the particular design. This will be done for the both primary and secondary windings of the transformer. Also it can wind multiple parallel windings at once, hence saving cost.

For primary - secondary isolation transformer, insulation is required in between the primary winding and the secondary winding. Generally the exposed enamel copper wire is protected by outer wrapping insulation tape for safety purpose. Normally all the insulations are done based on the creep and clearance distance requirements coming under IEC 61558 standard.

Toroidal transformer will not require a winding bobbin like with the laminated construction, but core insulation will act as a bobbin, which is creating better coupling of flux in the core together with the windings.

Toroidal construction is not much common and not popular in the industry due to its manufacturing complexity and high cost. However toroidal components can be seen in high end applications regardless of its high costs due to their high performance requirements.

Figure 1.2 shows a single-phase toroidal transformer which goes to a power supply unit for high-end audio amplifier.

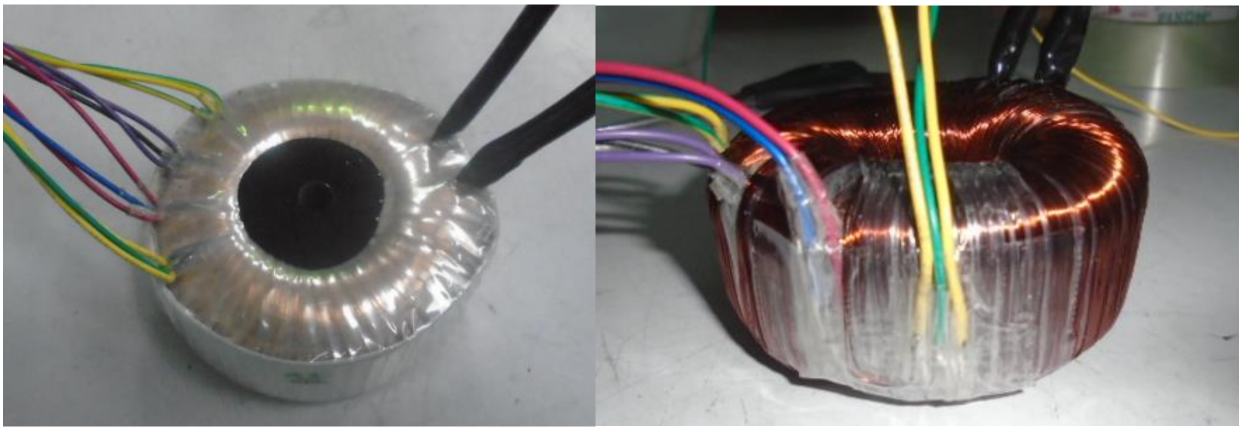

Figure 1.2: Toroidal transformer

Widely used transformer construction is laminated type transformers due to its simplicity in construction. A typical laminated type transformer is illustrated in Figure 1.3. When comes to low power transformers, most of the laminated type transformers are made with EI shaped core laminations. These are stamped as English letters ‘E’ and ‘I’ and these E’s and I’s are then stacked to form the core. Then the copper wire winding is done on a bobbin, and the wound bobbin is then inserted into the stacked E sections and then the I section will fixed on top of it.

Figure 1.3: EI laminated transformer

1.2 Motivation to the Research

Toroidal transformer has its advantages over laminated transformers of high efficiency, low weight, low leakage and low Electro Magnetic Interference (EMI), low volume, etc. The core loss in a toroidal transformer is very low since its gapless round shape, and which supports and allows the magnetic flux to travel ideally in a less reluctance magnetic path with minimum stray field. As a result, when designing toroidal transformers, the designers can go for high design flux densities and utilise material effectively than in laminated type [1].

However due to its low reluctance to flux, toroidal transformer exhibits severe inrush currents than standard laminated type transformers. This is one major drawback in toroids and it becomes worst when it comes to high power transformers. The situation gets worsen when higher quality grade steel is used, due to even low reluctance in the core to the flux.

High quality grain-oriented silicon steel (GOSS) has steep induction curve against excitation current and also they do have higher residual flux (remanence flux) which cause high inrush of the transformer.

Presently there are many methods to limit inrush current on toroidal transformers, both using external equipment based and transformer-based solutions. But most of the existing transformer-based mitigation methods are weakening the performance indicators of the toroidal transformer design; even it is more reliable than the external equipment based inrush current mitigation methods [1].

Therefore still there is an industry requirement to search for a more developed and optimized inrush mitigation method to boost the market share on toroidal transformers.

1.3 Objective of the Research

The main objective of this research is to develop a reliable and economical transformer-based inrush current mitigation method for toroidal transformers, which is compatible with the srilankan manufacturing facility. The conceptual proposal would be to use a slotted core which has a slot at the outer periphery of the steel core.

Using the proposed slotted core method, it is supposed to limit inrush current while maintaining its performance . With this method, it is expecting to save material costs and labour on the product and overall being competitive in the market.

The ultimate goal of the project is to promote toroidal transformers in the industry over other types of transformers, even in the high power levels.

INRUSH CURRENT IN TOROIDAL TRANSFORMERS

As mentioned in chapter 1 above, inrush current is a main problem for toroidal transformers than laminated transformers, especially considering high power levels. A brief introduction to toroidal transformers is provided in chapter 1 ,Here we will discuss the following key topics to better understand inrush current scenarios using toroidal transformers.

1) Theoretical background of inrush current
2) Toroidal core
3) Saturation inductance and inrush current

2.1 Theoretical Background of Inrush Current

This is a transient scenario, where high saturation of the transformer core originates high inrush current at the point of energization. There are several explanations on this scenario in several sources, but the below will illustrate the basics of the inrush current occurrence in a much clearer way.

Basically the input voltage applied to the transformer will be the driving force to the inrush current and that will force the flux to build up double the steady state flux plus the remanence flux. Hence the transformer gets in to deep saturation and that result with creating a high energization current [3].

Inrush current occurrence of a transformer is a transient effect which could be explained with electromagnetism as described follows.

The inrush current phenomenon is governed by Faraday's law [3].

$$\mathrm{v(t)} = \frac{d}{dt}\phi'(\mathrm{t}) \qquad (2.1)$$

Where v(t) is the instantaneous voltage applied and ϕ'(t) is the instantaneous flux linkage.

Then, $$\phi'(\mathrm{t}) = \int_0^t v(t)\, dt \qquad (2.2)$$

Neglecting the leakage flux component, the total instantaneous flux Φ(t) of the core with N number of turns of the winding can be written as,

$$\phi'(\mathrm{t}) = N\phi(\mathrm{t}) \qquad (2.3)$$

Then with combining equations (2.2) and (2.3)

$$\phi(\mathrm{t}) = \frac{1}{N}\int_0^t v(t)\, dt \qquad (2.4)$$

Consider the supply voltage for the transformer is sinusoidal with switching angle θ

$$\mathrm{v(t)} = V_m.\ \sin(\omega t + \theta)$$

Then re-write equation (2.4) with sinusoidal supply voltage v(t)

$$\phi(\mathrm{t}) = \frac{1}{N}\int_0^t V_m.\sin(\omega\mathrm{t} + \theta)\, dt \qquad (2.5)$$

$$\phi(\mathrm{t}) = \frac{V_m}{N}\int_0^t \sin(\omega\mathrm{t} + \theta)\, dt$$

$$\phi(\mathrm{t}) = \frac{V_m}{N\omega}.\left[-cos\,(\omega\mathrm{t} + \theta)\right]_0^t$$

$$\phi(\mathrm{t}) = \frac{V_m}{N\omega}.\left[-cos\,(\omega\mathrm{t} + \theta) + cos\,\theta\right] + \phi(0)$$

Considering the remanence flux at t=0 is $\phi(0) = \phi_r$ (Remanence flux)

Then,

$$\phi(\mathrm{t}) = \frac{V_m}{N\omega}.\left[-cos\ (\omega\mathrm{t} + \theta) + cos\ \theta\right] + \phi_r$$

The maximum flux ϕ_{max} is generated at zero crossing of the input voltage applied; means $\theta = 0$

$$\phi_{max} = \frac{V_m}{N\omega}.\left[2\right] + \phi_r$$

$$\phi_{max} = \frac{2V_m}{N\omega} + \phi_r$$

$$\phi_{max} = 2\phi_m + \phi_r \qquad (2.6)$$

So it is proven that, the inrush transient forces the flux to build up double the steady state flux plus the remanence flux. This scenario can be illustrated in graphical form as per the Figure 2.1 [3].

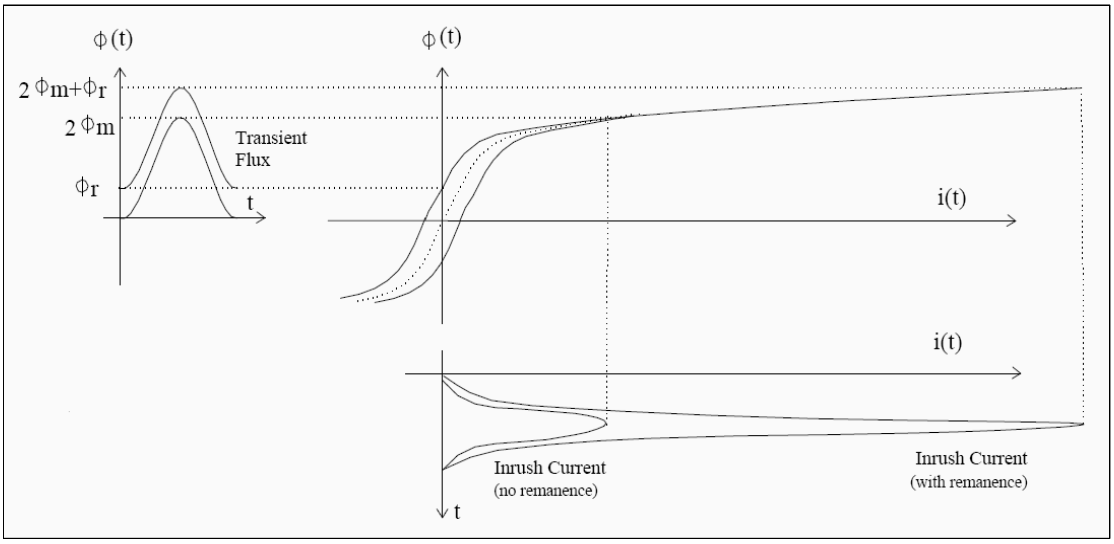

Figure 2.1: Graphical interpretation of Inrush current with remanence

2.2 Toroidal Core

Toroidal core is having donut shape with no air gaps in the magnetic path, against the laminated transformer cores. These cores are available in many material types; Silicon steel (SiFe), Nickel iron (NiFe), Perm-alloy, Nano-crystalline (NC) and others [1]. Silicon steel and nickel iron mainly available as tape wound cores or laminated pieces. In this research, only Silicon steel types are considered for toroidal transformer cores.

2.2.1 Silicon steel

Silicon steel is available as tape wound reels with different types/grades, thicknesses, widths and can be purchased based on the requirements of the relevant designs. Standard available steel widths are varying with the steps of 5mm, but still possible to purchase even other sizes in between, based on the demand. Figure 2.2 shows a silicon steel coil before the slitting process done, and in this form it is called as the ‘Mother coil’. Mother steel coil is commonly available with 350mm width.

Figure 2.2: Silicon steel mother coils

2.2.2 Silicon steel on toroidal core

Generally the silicon steel contains high permeability (μ) providing low reluctance (R) for a given Magnetic Path Length (MPL). When a transformer core is magnetized to the flux density (B) and the permeability increases as per following basic equation.

$$B = \mu . \mathrm{H} \qquad (2.7)$$

Where H – Magnetizing force

According to the BH characteristics of a typical silicon steel (see Figure 2.3), it maintains an almost linear relationship between B and H up to a certain magnetic flux density (which maintains maximum permeability), after which the steel is in the saturated region . Start to get closer. Hence, when the density of the magnetic flux increases further in the saturation region, the permeability decreases, approaching the values in the free space or in the air. This area is called the deep saturation of the core. This is a common scenario for all types of silicon steel, except for the difference in density of the magnetic flux where saturation begins.

Electrical steel comprises of various grades and have different classifications. One of the standard classifications is from its AISI grade. AISI stands for American Iron and Steel Institute [1].

Mainly the grain oriented steel type AISI M-5 is used for conventional low inrush designs to retain better performance, even together with fully air-gapped core. See Figure 2.3 for the steel characteristic curves taken from Kawasaki Steel data catalogue [4].

In this research also I have used M5 steel for the slotted core. Basically un cut area will be dominate at the normal operation and the slotted area will be dominate at the inrush condition.

2.3 Saturation Inductance and Inrush Current

In this research, it is proven that the most significant parameter affect to the inrush is saturation induction. In many literatures, they say the input winding resistance mainly affects the inrush current, but in practical scenario the designers do not have much allowance to change the winding resistances having a design is normally bound for particular temperature class.

Therefore in this research, the effects of saturation induction to the inrush current is mainly discussed and go through details on the inrush current variation by changing the slot depth of the outer periphery, hence changing the saturation induction.

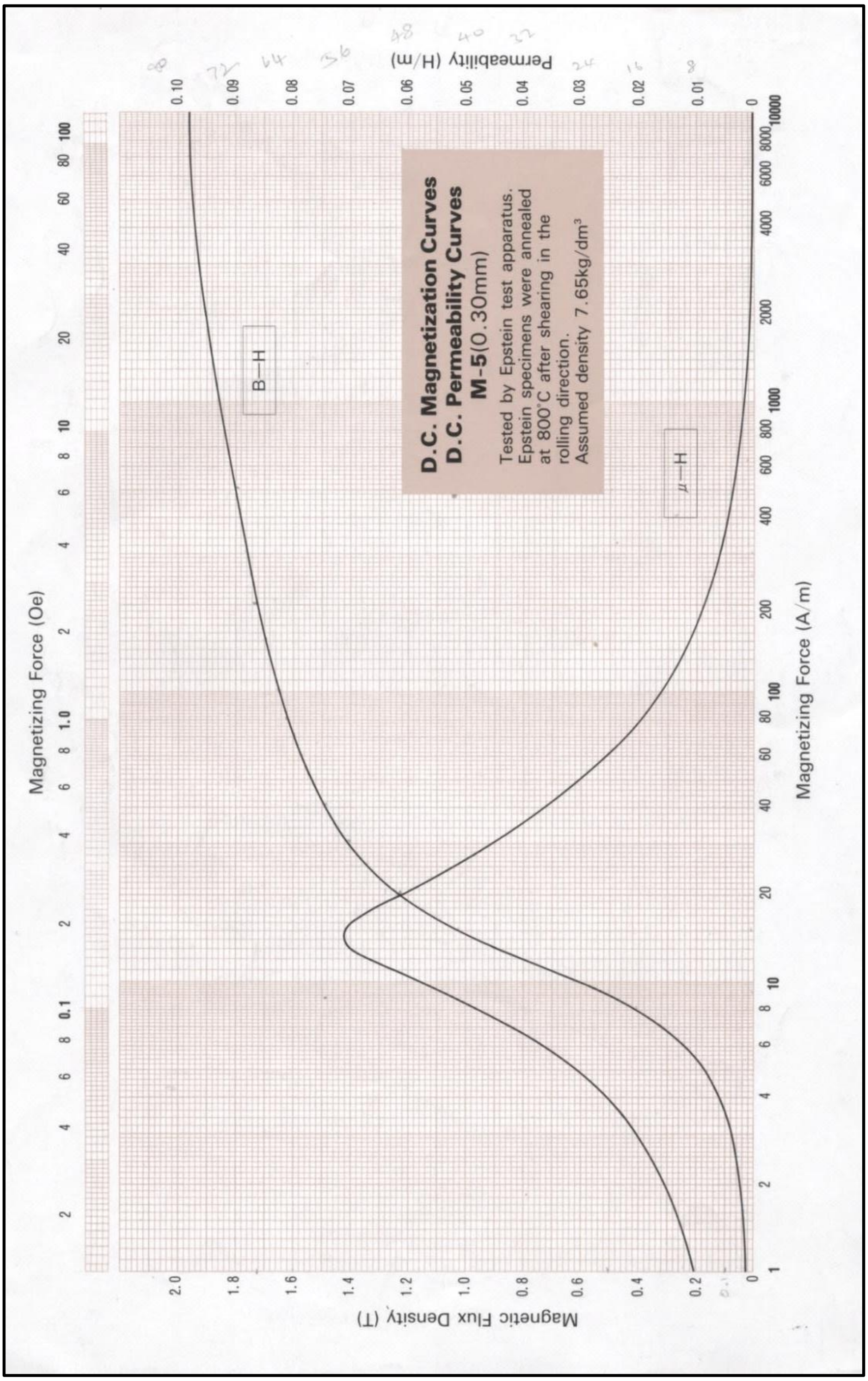

Figure 2.3 : BH characteristics for AISI M-5

RESEARCH DESIGN

In chapter 2, it was discussed about the inrush current phenomenon on toroidal transformers and about the factors that affect the magnitude of in rush transients; mainly the saturation inductance and electrical steel characteristics.

In this chapter following aspects are discussed descriptively.

1) Existing inrush current mitigation methods
2) Proposed slotted core concept for inrush current mitigation
3) Calculation of saturation inductance Ls
4) Calculation of inrush current

3.1 Existing Inrush Current Mitigation Methods

There are two main methods to mitigate inrush currents, those are external inrush control and others are transformer based in built inrush control systems.

Out of these two categories, most of the high end applications prefer the transformer-based solutions for inrush current mitigation, due to their higher reliability [1]. Followings are some of the methods used by designers/manufacturers for mitigation of inrush currents in toroidal transformers.

3.1.1 NTC thermistor in primary winding

The main advantage of this method is, here the transformer can be designed in higher flux density utilizing the magnetization curve to its maximum possible point. Also the transformer efficiency, weight, dimensions could also be to its optimum and also that lead avoiding complex manufacturing processes, hence finally be economical.
The Negative Temperature Coefficient (NTC) thermistors are thermally sensitive semiconductor resistors which exhibit inverse characteristic between the resistance and the absolute temperature, as shown in Figure 3.1. In typical operation of the NTC

thermistor, this is connected in series with the transformer input winding and initially holding high resistance at lower ambient temperature. But after the transformer is powered up, the resistance of the NTC thermistor can be brought down either by a change in the ambient temperature or by self-heating resulting from current flowing through the device [1].

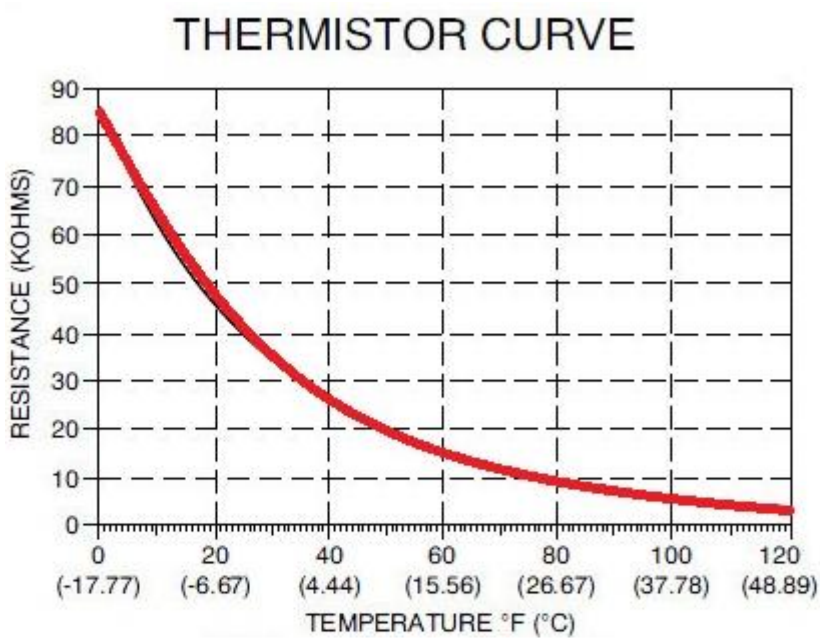

Figure 3.1: Typical characteristic curve for NTC

Referring the Figure 3.1, the x-axis is representing the temperature and the resistance by Y axis. That shows how the resistance drops with the temperature rise.

The main dis-advantages of this method are the addition of primary resistance to normal operation of the transformer and the heat dissipation and ultimately leading to low efficiency of the total equipment. And the next drawback is, it will not do the intended function in successive power interruptions, because due to the thermal inertia the thermistor may hold high temperature - low resistance stage in the next power up. The other drawback is the reliability. Transformer itself is highly reliable but adding the NTC thermistor in series with the supply makes the combination unreliable.

3.1.2 Use of NGOSS

The typical B-H curve for silicon steel presents steep magnetization characteristic after they exceed the maximum unsaturated flux density. This characteristic is far great especially with GOSS types, while it is not that much critical for NGOSS types.

Generally toroidal transformers are wound using high grade GOSS for its common intended performances, but the said steep magnetization curves of GOSS and high design flux density makes easy to saturate the core. See Figure 3.2 and Figure 3.3 for magnetization characteristics with corresponding loss curves for GOSS (AISI M-5) [4].

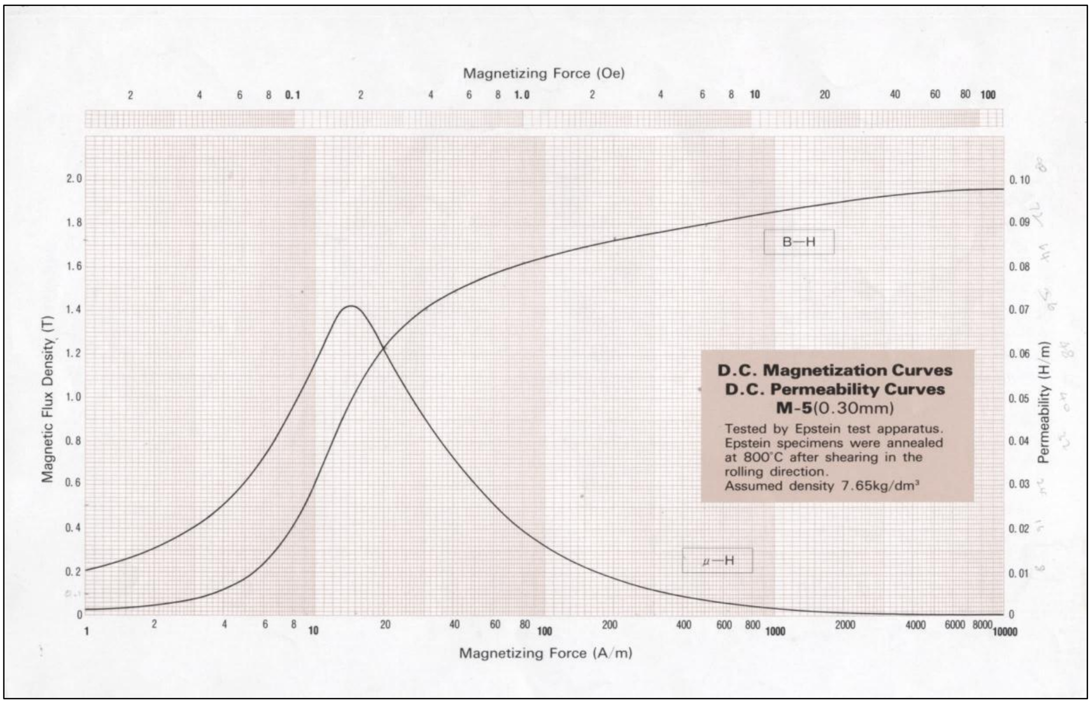

Figure 3.2: Magnetization characteristics for GOSS-AISI Grade M5

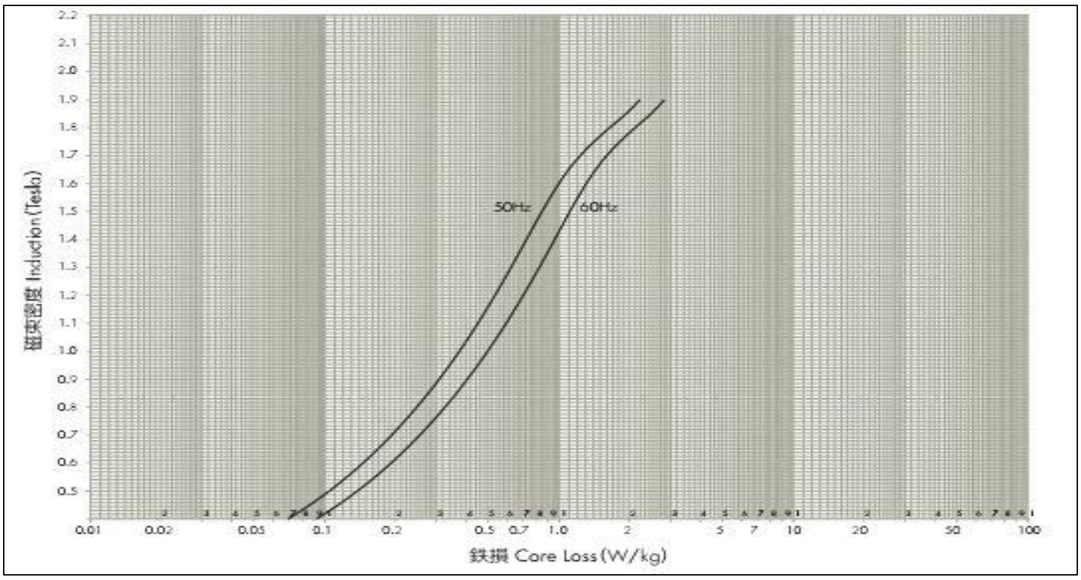

Figure 3.3: Core loss curve for GOSS-AISI Grade M5

As a result, designers are using NGOSS for low inrush designs due to lower steep characteristics in magnetization [1]. NGOSS transformers have to be designed in low flux density and then its narrow magnetization characteristics can be used to keep it unsaturated, compared to the GOSS types. Following Figures 3.4 to 3.5 illustrates magnetization characteristics with corresponding loss curves for NGOSS (35H300) [4], for easy understanding of above mentioned point.

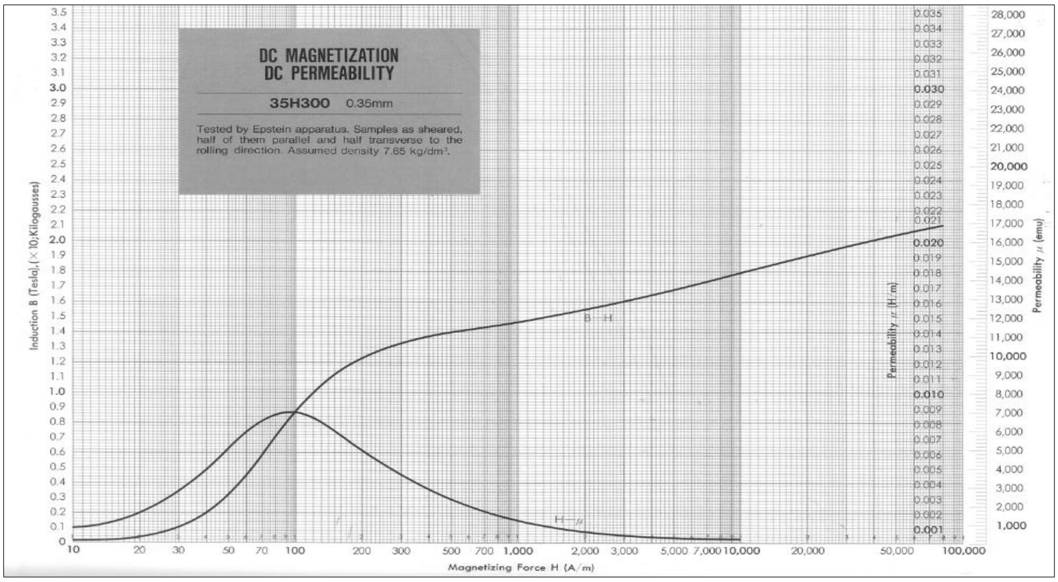

Figure 3.4: Magnetization characteristics for NGOSS 35H300

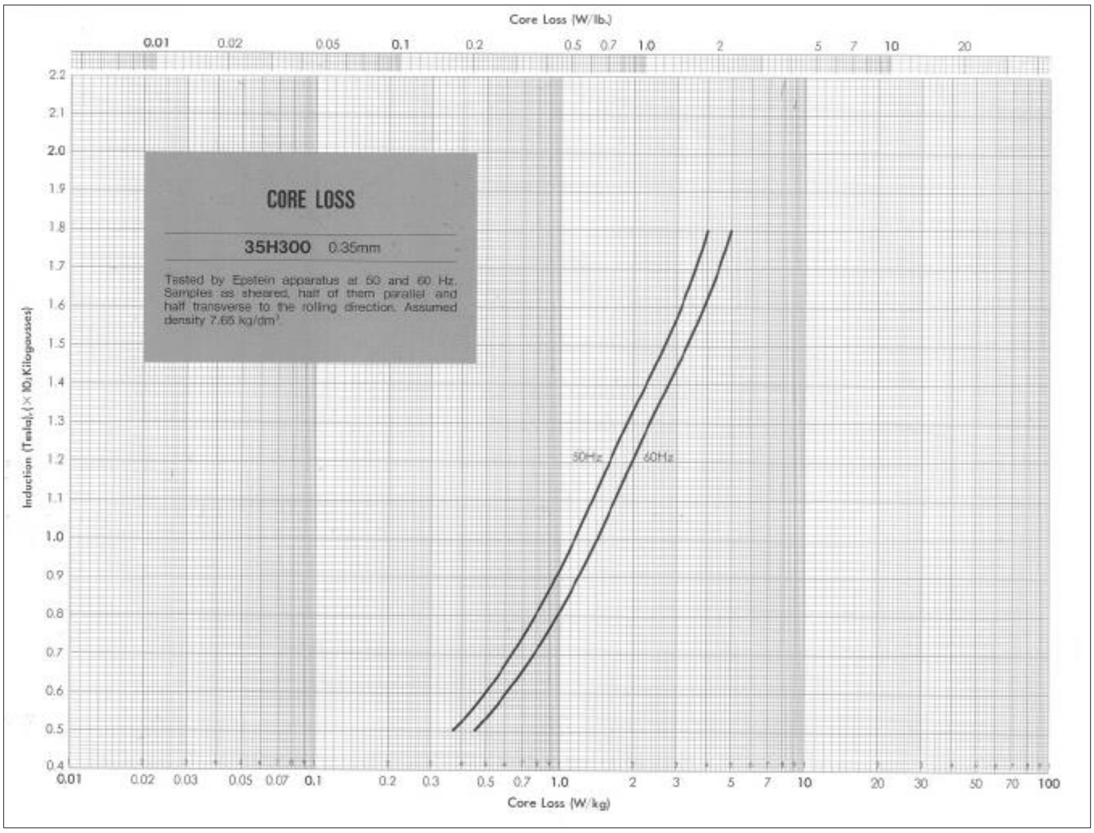

Figure 3.5: Core loss curve for NGOSS 35H300

Selection of NGOSS does reduce the inrush current to some extent, but when the application is critical on inrush current, the designers also tend to use above NGOSS without annealing process [1]. Annealing is a special heat treatment process done to regain the magnetic properties back to steel core, after it has been lost in the core manufacturing process.

The main drawback of this method is the less efficiency of the transformer due to high core losses (see Figure 3.5) and high excitation current. These designs are obviously bulky and weight is more than the standard GOSS designs.

However reliability point of view this method is better than the method described in previous section 3.1.1.

3.1.3 Cut core toroidal transformers

Introducing a cut (or a small air-gap) to the magnetic path of the toroidal core will change magnetization characteristics of the steel; basically this will increase the unsaturation characteristic even at the high flux densities. Based on the BH characteristics, it will reduce the slop of the curve (or reduce permeability) and bring the knee point to the right side of magnetization curve, while increasing the magnetizing force.

Also the other main purpose is reducing the remanence flux (ϕ_r). As per the equation 2.6 derived for inrush current (also Figure 2.1), the remanence flux (or remanence flux density, B_r) plays an important role in the inrush current. The Figures 3.6 illustrates how the remanence flux density get reduced (by ΔB) together with an air gap in the toroidal core [5].

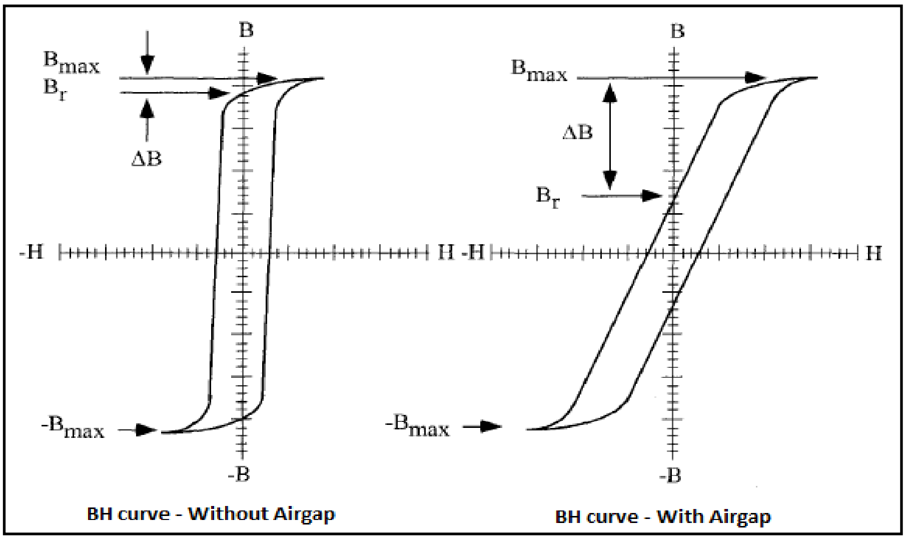

Figure 3.6: BH loops before and after core cut

There are several advantages and disadvantages of this method.

An advantage of this method is, this method does not change the core losses with respect to the uncut core. Note in Figure 3.6, the areas within the BH loops for with and without air-gap are almost same.

Also this inrush mitigation method is more reliable than the external NTC thermistor option described in previous section 3.1.1.

Regarding the disadvantage; the gapped cores need more Magneto Motive Force (MMF) to magnetise the core than the normal toroidal core, hence it draws higher current in the off-load condition. Due to that reason, the gapped core transformer consumes lot more reactive power loss. Therefore this cannot be designed at its optimum flux density and hence should be designed approximately 30% lower value. Also core vibration due to loose lamination and noise issues could be an issue in the end application [1].

Based on the discussed inrush current mitigation methods, the gapped core option is mostly used in applications due to its reliability and other advantages. But still it is necessary to overcome its disadvantages, and hence the slotted core method introduced with this research.

3.2 Proposed Slotted Core Concept for Inrush Current Mitigation

3.2.1 Scope of the Research

Together with the discussions this research will be confined into the following scope.

1) Design flux density varied from 0.9T to 1.6T and experiments conducted only for 230V mains input.
2) Slot width kept constant as blade thickness of 1.5mm
3) Slot depth varied as 5, 10, 15, 20, 25mm.
4) Considered only the steel types M5 steel.
5) Considered transformer power range 1kVA

3.2.2 Methodology

In this method, a slot will be added to the outer periphery of the toroidal core as below. As discussed in the previous chapter, what we supposed to control is the saturation inductance of the core, hence the inrush current.

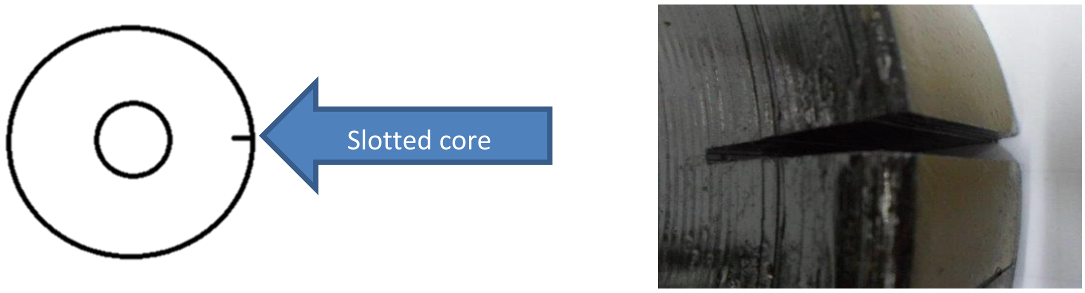

Figure 3.7: Slotted core

Here the thickness of the slot will be constant as the cutting blade thickness.
And the slot depth will be varied throughout the research in order to get the optimum value.

3.2.3 Simulation of flux distribution

In toroidal transformers, centre of the core will be magnetized at the no load condition, as in below FEMM simulation. As per the theory the majority of flux will concentrate on the lowest magnetic path length (means close to the inner core),

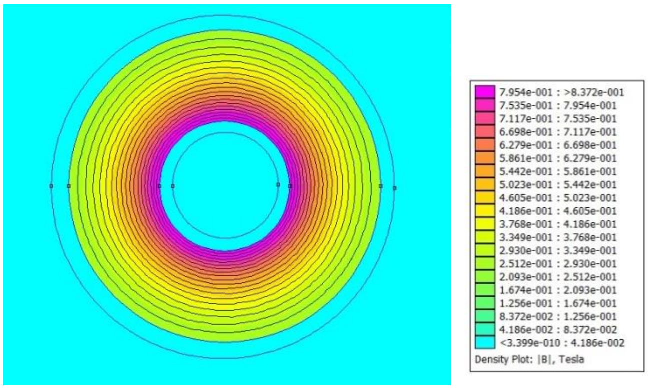

Figure 3.8: No load condition

But at the inrush condition , flux will be distributed in the complete core and the core will get saturated. That inrush condition also can be simulated as below.

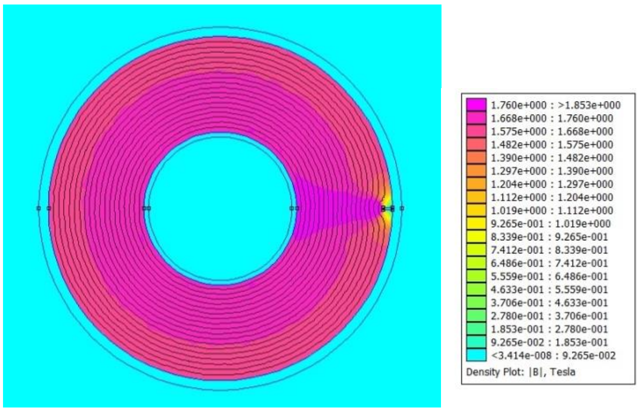

Figure 3.9: Inrush condition

3.2.4 Development of slotted core

Toroidal core has made with a steel strip wound on a circular bobbin. So before the core cutting, first of all core varnishing has to be done to avoid peel off strips.
In order to make this slot , existing core cutting machines (Band saw machines) has to be modified with circular saw and need a special jig for slot cutting.

Figure 3.10: Machine modification for slot cutting

Without this machine modification we cannot cut the slot because the existing band saw can cut only full way through the complete core. So this modification is essential to avoid practical issues with slot cutting.

Then finally slot cutting can be done as below Figure 3.10 .

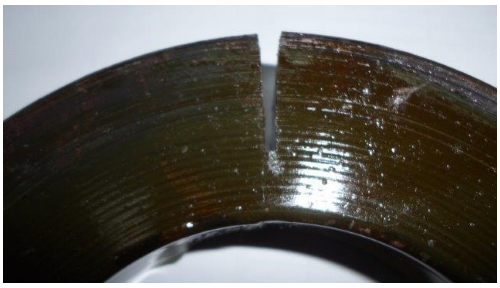

Figure 3.11: Slotted core

Then as per the research scope , slot depths are made for 5 levels as below.
(5,10,15,20,25mm depths)

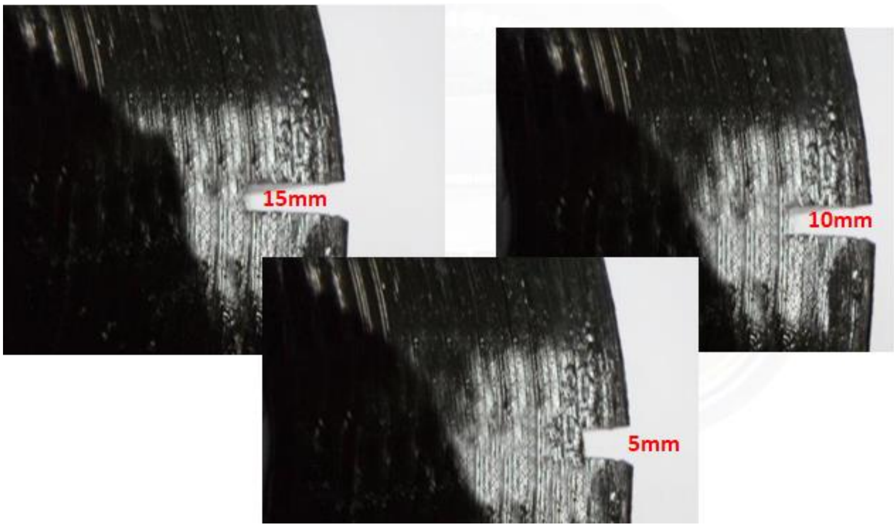

Figure 3.12: Different slot sizes

3.2.5 Transformer winding

In this research transformers were designed for 1.6T flux density and throughout the research flux density will be changed for 8 levels 0.9T to 1.6T by increasing no of turns for inrush testing.

When considering 5 different slot depths and 8 flux densities, all together 40 samples will be tested for inrush current.

Figure 3.13: Sample windings

3.2.6 Theoretical inrush calculation

Slot depth is the main design parameter in designing process with slotted core designs. First, the equation 3.1 is showing the general relationship between the maximum inrush current and the impedance of the product [6] [7].

$$I_{max} = \frac{V_m}{\sqrt{(\omega L_s)^2 + R^2}} \,.\, (1 + cos\,\theta + \frac{B_s - B_r}{B_n}) \qquad (3.1)$$

I_{max} - Maximum inrush current (peak current)
V_m - Maximum input voltage (peak voltage)
R - Winding resistance
L_s - Saturation inductance
θ - Switching angle
B_r - Residual flux density
B_s - Saturation flux density
B_n - Nominal design flux density

According to the equation 3.1, it is obvious that increasing the Saturation inductance (L_s) and Winding resistance (R) will be the main option to minimize the inrush current. When comes to winding resistance, in practical situation the designer does not have much allowance to changed resistance having the product itself should complied with certain thermal class. Hence changing the winding resistance is not an option to control the inrush current. Therefore, increasing the Saturation inductance will be the only option in this regards.

So in this case when the slot depth will be increased, saturation inductance increases.

But at some point it will be effect for the core saturation and it counter effects to increase inrush current. So there will be an **optimum depth** for a transformer to meet the specified inrush current.

The following test has been done to the 1000VA transformer, where the inrush current is measured with different slot depths.

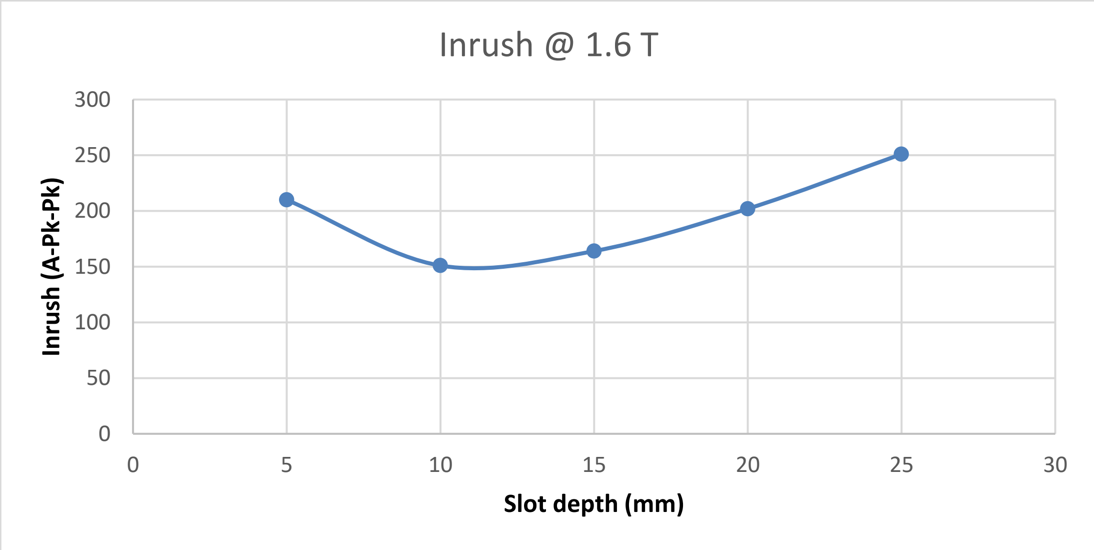

Figure 3.14: 1.6T flux sample test results

With the above test results we can see that for a particular flux density there is an optimum slot depth where we can have the minimum inrush current.

Since the inrush current depends on the flux density, the experiment has followed for 8 levels of flux densities.

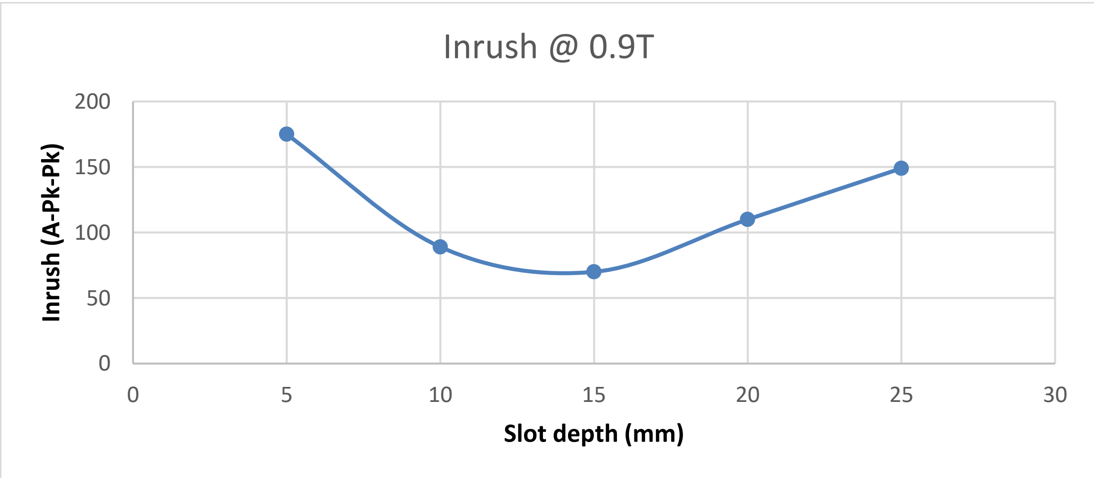

Figure 3.15: 0.9T flux sample test results

Above is the test result for different gap sizes, for 0.9T flux density. There we can see the effect of flux density for the inrush current of the transformer.

This flux density was changed by increasing no of turns of the already wound samples. Even at that lower flux, the inrush curve shows that there is an **optimum slot depth** for the minimum inrush. Here below is the test result for the 40 samples.

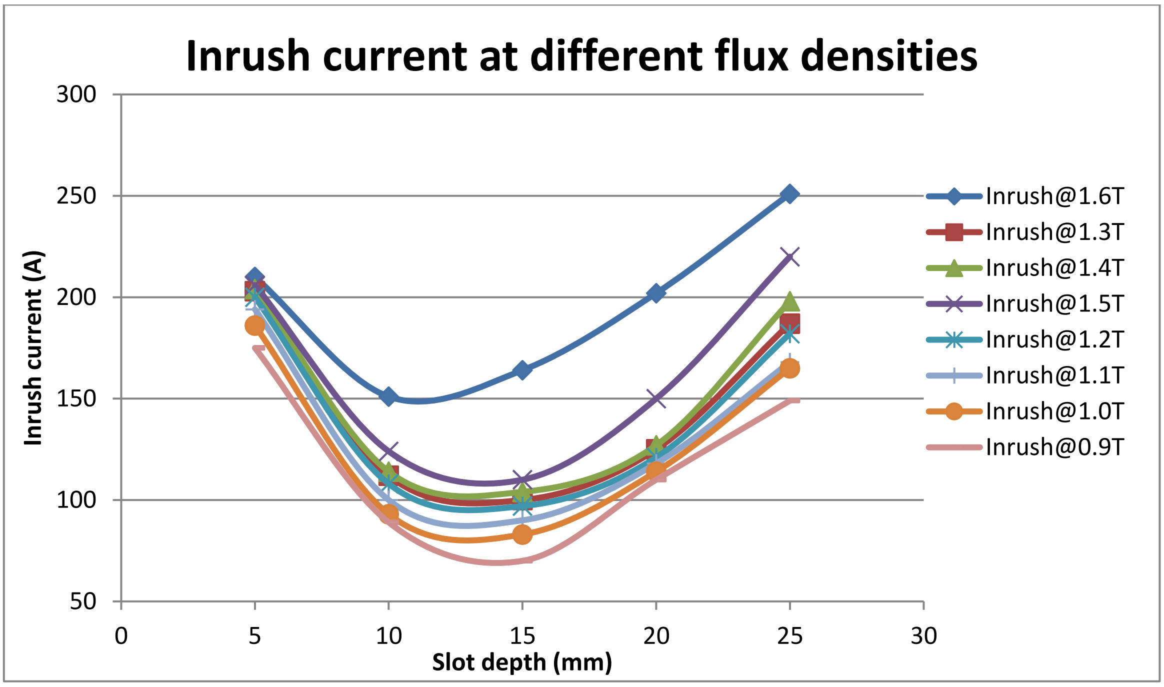

Figure 3.16: Sample test results

By analysing above test results, we can see that we can control the inrush current by controlling the design flux density and the slot depth. So according to the customers requirement we can select those figures and get the optimum design output.

3.3 Calculation of saturation inductance Ls

According to the concept, as the slotted core subjected to deep saturating condition, the outer slotted area will retain in the “Just unsaturated” stage, while the centre uncut core area will be saturated.

Hence the inductance of the **inner uncut core area** can be considered as the inductance of saturated core (air choke).

$$L_{uncut} = \frac{4\pi \text{ x } 10^{-7} \,.\, N^2 . A . \mu_r}{\mathrm{MPL}_{uncut}} \qquad (3.2)$$

L_{uncut} - Saturated Inductance of the inner uncut core area.
A - Cross sectional area of core
μ_r - Relative Permeability
MPL - Magnetic path length
OD/ID – Outer/Inner diameter of core
N - Number of turns

Where MPL is calculated by,

$$MPL = \frac{\pi \text{ x } (\mathrm{OD} - \mathrm{ID})}{\ln(\frac{OD}{ID})}$$

Considering the 1000VA transformer, with 10mm slot depth and total core size 180 x 75 x 35.

Uncut core dimension (OD x ID x H)	: 160 x 75 x 35 mm
Cut core dimension (OD x ID x H)	: 180 x 160 x 35 mm
Number of turns	: 371 turns

The parameters for the centre “uncut core”;

Saturated (uncut) core area	= 1399.24 mm^2
Relative permeability	= 1 (Air)
MPL	= 351.40 mm

Substituting the uncut core data into equation 3.2

$$L_{uncut} = 0.6887mH$$

Then the inductance of the **outer slotted core area** can be calculated from the equation 3.3

$$L_{cut} = \frac{4\pi \times 10^{-7} N^2 A.\mu_r}{MPL + \mu l_g} \qquad (3.3)$$

L_{cut} - Slotted area un-saturated Inductance
l_g - Air gap

The parameters for the slotted area.

Un-saturated Slotted core area	= 1350 mm^2
Relative permeability	= 102.00
MPL	= 532.09 mm
Air gap	= 1.5 mm

Substituting the cut core data into equation 3.3

$$L_{cut} = 0.0089H$$

Then the total Saturation inductance L_S is;

$$L_S = L_{uncut} + L_{cut}$$
$$L_S = 0.0096H$$

It shows that the inductance of the uncut saturated core area (L_{uncut}) is negligible on the resultant inductance $\boldsymbol{L_S}$, and hence on the inrush current.

3.4 Calculation of inrush current

Recall the equation 3.1

$$I_{max} = \frac{V_m}{\sqrt{(\omega L_s)^2 + R^2}} \cdot \left(1 + \cos\theta + \frac{B_s - B_r}{B_n}\right) \qquad (3.1)$$

Having this research is concentrate only on the Maximum inrush current, which occurs at the zero crossing. Then apply θ = 0

$$I_{max} = \frac{V_m}{\sqrt{(\omega L_s)^2 + R^2}} \cdot \left(1 + 1 + \frac{B_s - B_r}{B_n}\right)$$

$$I_{max} = \frac{V_m}{\sqrt{(\omega L_s)^2 + R^2}} \cdot \left(2 + \frac{B_s - B_r}{B_n}\right)$$

Also applying $V_m = \sqrt{2}\, V_{rms}$

$$I_{max} = \frac{\sqrt{2} V_{rms}}{\sqrt{(\omega L_s)^2 + R^2}} \cdot \left(2 + \frac{B_s - B_r}{B_n}\right) \qquad (3.4)$$

As per the experimental data, the value of $\frac{B_s - B_r}{B_n}$ stays almost constant, irrespective to the slot size. This is proven as following.

Consider the BH loops of two slotted core transformers of 1000VA, which are identical except having different slot depths of 10mm and 20mm.

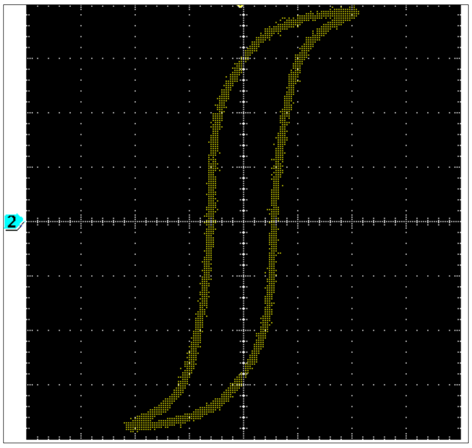

10mm slot

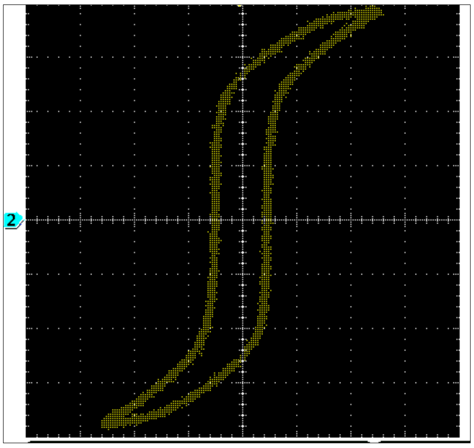

20mm slot

Figure 3.17: BH loops at different air-gaps

According to Figure 3.16, the change of the remanence flux is almost negligible even for high variation of slot size. Hence the ratio between the saturated flux density (B_s) and remanence flux density (B_r) is considered fixed as following, in this research.

Means, $B_r = 0.75\ B_s$

Therefore we can calculate,

$$B_s - B_r = 0.25\ B_s \qquad (3.5)$$

Then the slotted core is subjected to deep saturation level and studied its BH loop characteristics. Refer Figure 3.17.

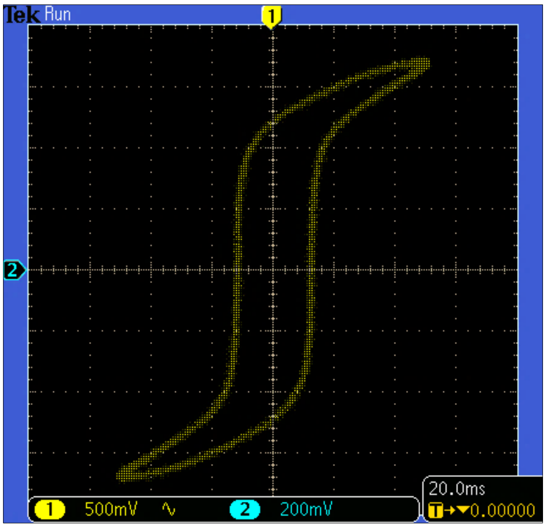

Figure 3.18: BH loop at deep saturation

Accordingly it is observed the design starts saturation when the nominal voltage gets nearly 2.5 times, means closer to 600V (230V nominal).

Therefore we can derive, $B_s : B_n = 2.5 : 1$ (3.6)

From equations (3.5) and (3.6), it is possible to derive,

$$\frac{B_s - B_r}{B_n} \approx 0.65 \qquad (3.7)$$

Then substituting the equation 3.7, into equation 3.4.

$$I_{max} = \frac{\sqrt{2}V_{rms}}{\sqrt{(\omega L_s)^2 + R^2}} \cdot (2 + 0.65)$$

$$I_{max} = \frac{3.75\ V_{rms}}{\sqrt{(\omega L_s)^2 + R^2}} \qquad (3.8)$$

Accordingly it is possible to calculate theoretical value for the I_{max} , together with the calculated saturation inductance L_s and calculated winding resistance (R = 0.635 Ω)

I_{max} = 243.12 A

But the measured inrush current under the laboratory facility will be vary from this value.The reason for this deviation is the line inductance for the test bench supply system.The source impedance to the transformer makes a great effect to the above deviation, over the other factors. So in order to correct it we have to do line inductance correction for the calculated inrush value.

By adding 0.006H as the line inductance correction, we will have the theoretical value

$$I_{max} = 151.67\text{A}$$

The actual value measured was 151A , which is almost equal for the theoretical value.

EXPERIMENTAL DATA COLLECTION

In chapter 3, slotted core method had been discussed together with 1000VA transformer. This chapter discusses on further details of experimental data collected for slotted core designs, which has slot sizes from 5mm to 25mm and flux densities from 0.9T to 1.6T. All together 40 samples were tested in order to identify the relationship between inrush current, flux density and slot depth.

4.1 Inrush Current Measurement on Samples

The transformers were tested applying alternating rated voltage 230V/50Hz across the primary winding. Then the inrush current transient waveforms are taken to an Oscilloscope (Tektronix DPO3000) connected via a current probe (Tektronix A621) to the circuit. Test set up for this arrangement is shown in Figure 4.1 [1].

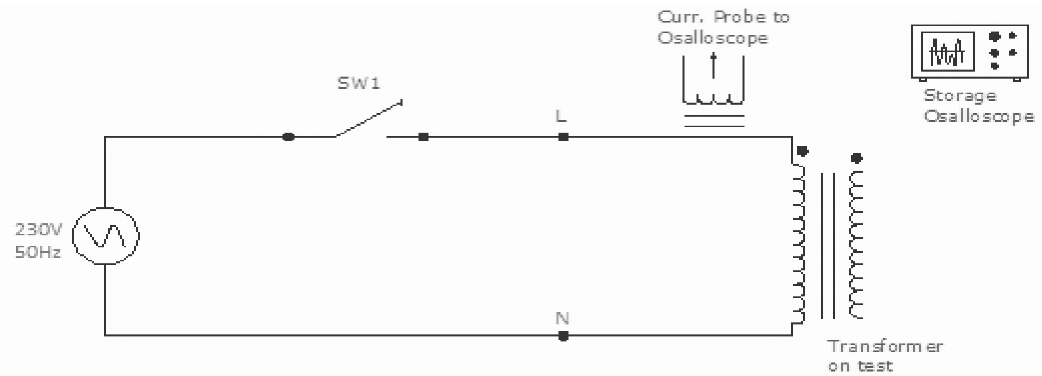

Figure 4.1: Test setup for inrush current measurement

In this experiment, the inrush current data collected with two methods. First method is repeating the test several times (minimum 60 times per design), creating the possibility to switch the input wave form at zero crossing, and hence creating the maximum inrush current. The second method is switching the input via zero-point detecting circuit (made with SIEMENS 3RF2050-1AA02), which does monitor and detect the zero crossing of the input wave form and ensure to switch ON the transformer at that point.

Both the options provided almost same maximum inrush current value, for each scenario to be discussed in section 4.2.

4.2 Finding the optimum slot depth or the minimum inrush current.

In this case, each design was tested for inrush current, varying slot depth and the flux density. Here optimum slot depth will be the minimum slot depth which can get at a higher flux density. Since core cutting time directly reflects to the manufacturing cost and because transformer size depends on the flux density, we can choose the optimum slot size with those two parameters. Here below are the test results for 40 samples.

Table 4.1: 1.6T sample test results

Sample No	Slot	A (Slot)	Flux	Turns	Inrush@1.6T
8	25	1312.5	1.6	371	251
16	20	1050.0	1.6	371	202
24	15	787.5	1.6	371	164
32	10	525.0	1.6	371	151
40	5	262.5	1.6	371	210

Table 4.2: 1.5T sample test results

Sample No	Slot	A (Slot)	Flux	Turns	Inrush@1.5T
7	25	1312.5	1.5	396	220
15	20	1050.0	1.5	396	150
23	15	787.5	1.5	396	110
31	10	525.0	1.5	396	124
39	5	262.5	1.5	396	206

Table 4.3: 1.4T sample test results

Sample No	Slot	A (Slot)	Flux	Turns	Inrush@1.4T
6	25	1312.5	1.4	424	198
14	20	1050.0	1.4	424	127
22	15	787.5	1.4	424	104
30	10	525.0	1.4	424	114
38	5	262.5	1.4	424	204

Table 4.4: 1.3T sample test results

Sample No	Slot	A (Slot)	Flux	Turns	Inrush@1.3T
5	25	1312.5	1.3	457	187
13	20	1050.0	1.3	457	125
21	15	787.5	1.3	457	100
29	10	525.0	1.3	457	112
37	5	262.5	1.3	457	203

Table 4.5: 1.2T sample test results

Sample No	Slot	A (Slot)	Flux	Turns	Inrush@1.2T
4	25	1312.5	1.2	495	182
12	20	1050.0	1.2	495	121
20	15	787.5	1.2	495	97
28	10	525.0	1.2	495	108
36	5	262.5	1.2	495	200

Table 4.6: 1.1T sample test results

Sample No	Slot	A (Slot)	Flux	Turns	Inrush@1.1T
3	25	1312.5	1.1	540	168
11	20	1050.0	1.1	540	118
19	15	787.5	1.1	540	90
27	10	525.0	1.1	540	100
35	5	262.5	1.1	540	194

Table 4.7: 1.0T sample test results

Sample No	Slot	A (Slot)	Flux	Turns	Inrush@1.0T
2	25	1312.5	1	594	165
10	20	1050.0	1	594	114
18	15	787.5	1	594	83
26	10	525.0	1	594	93
34	5	262.5	1	594	186

Table 4.8: 0.9T sample test results

Sample No	Slot	A (Slot)	Flux	Turns	Inrush@0.9T
1	25	1312.5	0.9	660	149
9	20	1050.0	0.9	660	110
17	15	787.5	0.9	660	70
25	10	525.0	0.9	660	89
33	5	262.5	0.9	660	175

All together we can analyse test results as in Figure 3.16

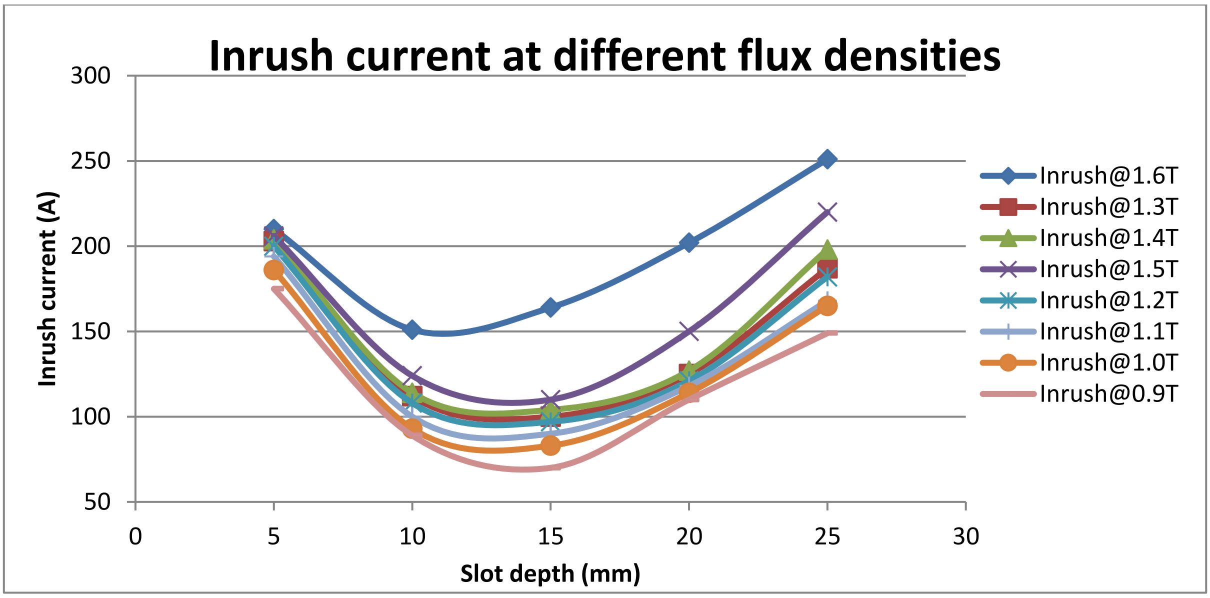

Figure 3.16: Sample test results

ANALYSIS OF DATA

In this chapter, it is mainly focused to build up a methodology to calculate inrush current towards developing a design tool. As discussed in chapter 3, basically the equation 3.1 can be used for inrush calculation. But together with the experimental data collected in chapter 4, there are certain characteristics can be built and embedded in to the calculation towards handling the design parameters.

In this chapter the following aspects will be discussed together with the data obtained in chapter 4 and the inrush current calculation method discussed in the chapter 3.

1) Theoretical inrush calculation
2) Optimum slot depth calculation for a specified inrush current.
3) Design tool development.

5.1 Theoretical inrush calculation.

As discussed in chapter 3, below equation (5.1) can be uses for theoretical inrush calculation. As input parameters we have operating voltage (Vrms) , winding resistance (R) and saturation inductance(L_s) calculated according to the slot depth and core size as discussed in chapter 3.

$$I_{max} = \frac{3.75\, V_{rms}}{\sqrt{(\omega L_s)^2 + R^2}} \qquad (5.1)$$

5.2 Optimum slot depth calculation for specified inrush current

Using experimental data collected as explained in chapter 4 , we can derive these equations for different flux densities.

X= Slot depth

Y= Inrush current

Flux(T)	Equation for inrush with gap
1.6	$y = 0.0022x^4 - 0.1727x^3 + 5.245x^2 - 64.383x + 421$
1.5	$y = -0.0007x^4 + 0.0147x^3 + 1.3367x^2 - 37.767x + 360$
1.4	$y = 0.0041x^4 - 0.2693x^3 + 7.0967x^2 - 85.067x + 483$
1.3	$y = 0.0028x^4 - 0.196x^3 + 5.71x^2 - 74.8x + 457$
1.2	$y = 0.0032x^4 - 0.2213x^3 + 6.26x^2 - 79.567x + 467$
1.1	$y = 0.002x^4 - 0.1613x^3 + 5.27x^2 - 73.367x + 448$
1	$y = 0.0014x^4 - 0.126x^3 + 4.565x^2 - 67.65x + 425$
0.9	$y = -0.0035x^4 + 0.1627x^3 - 1.3733x^2 - 18.567x + 284$

Here we can observe the trend will be differ with the design flux. And depending on the design flux we can choose the relevant trend for the relationship of the slot depth and inrush current. Here there will be two slot depths for a specific inrush value.

When considering manufacturing costs, the lowest slot depth will be the optimum value for the specific flux density.

5.3 Development of Design Tool for Slotted Core

This section will discuss on development of a design tool for slotted core, integrating the equations and characteristics derived in the previous sections.

As discussed in the chapter 3, all the designs considered in this research are done for 1kva transformers which has different design flux densities and different slot depths. Hence in this design tool the designer will only need to input the core dimensions , primary voltage and number of turns. Then the tool will calculate design flux by itself. Also we have to enter primary resistance which we can get from the toroid design tool. The Figure 5.1 shows the simplified flow chart for the calculation tool.

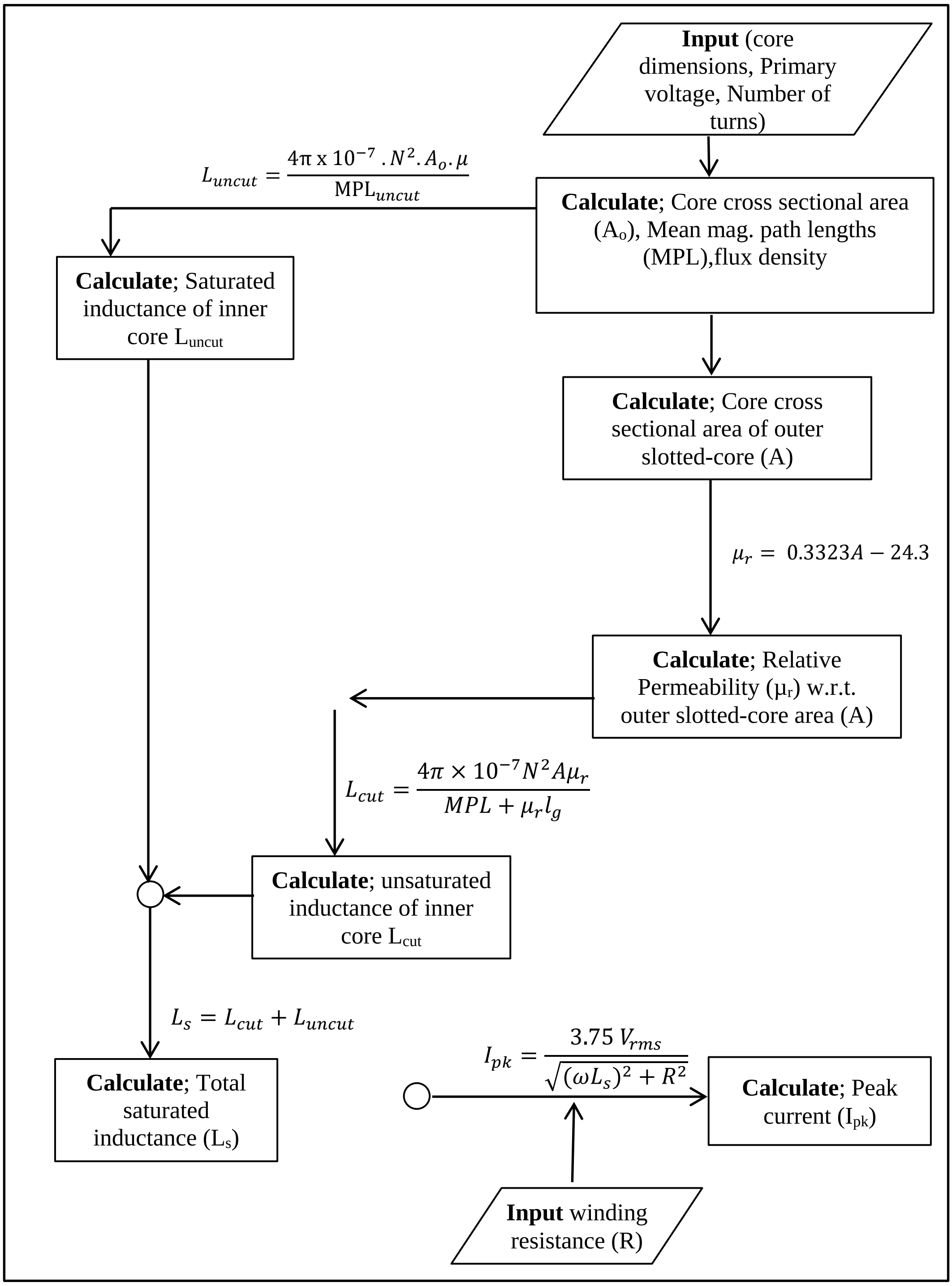

Figure 5.1: Flow chart of Design tool

Then the flow chart can be presented as a design tool, which can be programmed with different software programming languages. The following Figure 5.5 is showing the program which is done on the Flow chart, with Microsoft Excel .

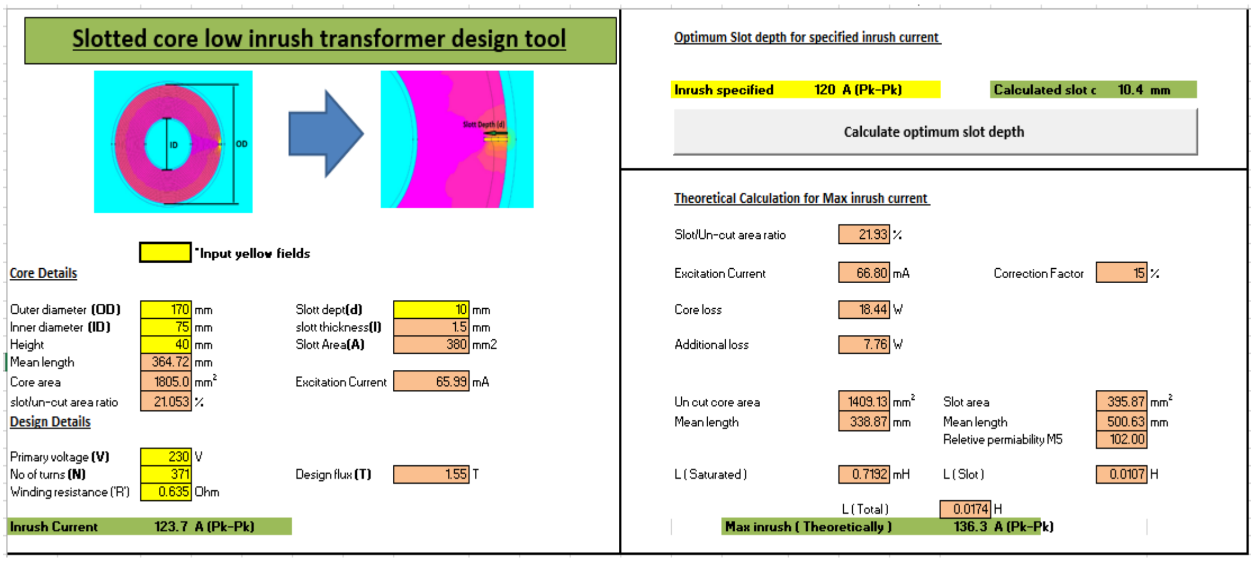

Figure 5.2: Design tool

As shown in the Figure 5.2, the designer will only have to input only the dimensions of the cores and the resistance of the input winding, and the design tool will calculate the optimum slot depth according to the customer specified inrush current which designer has to meet at the end.

5.4 Design tool validation

In this section, it shows the performance of the developed tool comparing together with the measured inrush current values. Three samples were done for design tool validation and these samples were manufactured according to the design tool outcome.

Sample 1:- Customer specified inrush is 120A pk-pk , for 1KVA t/x.

- New core dimensions will be
  OD 170mm ,ID 75mm , H 40mm
- According to the tool , optimum slot depth = 10.4mm
- According to the tool, theoretical maximum inrush current will be
  136A pk-pk .

Measured inrush value= 116A pk-pk

Sample 2:- Customer specified inrush is 150A pk-pk , for 1KVA t/x.

- New core dimensions will be
  OD 180mm ,ID 85mm , H 40mm
- According to the tool , optimum slot depth = 7.9mm
- According to the tool, theoretical maximum inrush current will be
  165A pk-pk
- Measured inrush value= 136A pk-pk

Sample 3:- Customer specified inrush is 180A pk-pk , for 1KVA t/x.

- New core dimensions will be
  OD 190mm ,ID 95mm , H 40mm
- According to the tool , optimum slot depth = 6.2mm
- According to the tool, theoretical maximum inrush current will be
  191A pk-pk
- Measured inrush value= 173A pk-pk

It is observed that there is only a small deviation between the calculated and measured inrush current values. Means it is evident that the characteristic equations built up for inrush calculation is with high accuracy towards calculating inrush current.

Also it is noted that the deviations are always positive, means the calculated inrush current values are always higher, than the measured inrush current values.

One of the main reasons for that will be the source impedance , which will never be zero in real applications. Note, the above measured values are taken from a source with very low impedance, hence the deviations are minimal. Therefore considering calculated values as the maximum inrush current is obviously safe, considering all the applications.

Meantime the inrush current values shows that the slotted core method does have a good control over the inrush current value, rather than the conventional transformer based inrush current mitigation methods. Hence it can be concluded that, together with the slotted core method, it is possible to calculate the inrush current values within 10%, including the manufacturing tolerances.

5.5 Comparison of electrical performance with conventional inrush mitigation method.

Table 5.1: Electrical parameters comparison

Normal core(170*75*40, M5)	**Cut core(170*75*40, M5)**	**Slotted core(170*75*40, M5 , 10.4mm slot)**
Inrush measured = 210 A pk-pk	Inrush measured = 112 A pk-pk	Inrush measured = 116 A pk-pk
Core loss = 17W	Core loss = 25W	Core loss = 23W (improved by 2W)
Voltage regulation = 6%	Voltage regulation = 10%	Voltage regulation = 8% (Regulation improved)
No load current = 68 mA	No load current = 84 mA	No load current = 78mA (improved by 6mA)

When comparing with other transformer based inrush mitigation methods, here it is observed there are lot of improvements in performance while having a good control in inrush current.

5.6 Comparison of manufacturing cost with conventional cut core method.

- Huge saving on core manufacturing cost over cut core method.
    - 3 days of glue curing time is eliminated
    - Core cutting time 2.5mm/min improved to 3.2mm/min (hence reduces machine time and labour time)
    - Gluing process has eliminated (Save labour and material)
    - No need steel bands to keep tight the core

Table 5.2: Conventional cut core costing

Conventional Cut-core				
Description	Unit	Unit price(USD)	Qty	Cost(USD)
Copper	kg	8.3	1.05	8.72
M5 steel	kg	2.40	3.12	7.49
Glue LOCKTITE	g	0.07	15.00	1.11
Steel band	pcs	1.10	2.00	2.20
Material Cost				19.51
Machine cost (35mm cut @ 2.5mm/min)	min	2.30	14.00	32.20
Total cost				**51.71**

Table 5.3: Slotted core costing

Slotted core				
Description	Unit	Unit price(USD)	Qty	Cost(USD)
Copper	kg	8.3	1.05	8.72
M5 steel	kg	2.40	3.12	7.49
Glue LOCKTITE	g	0.07	0.00	0.00
Steel band	pcs	1.10	0.00	0.00
Material Cost				16.20
Machine cost (10mm cut @ 3.2mm/min)	min	2.30	3.13	7.19
Total cost				**23.39**

With the proposed slotted core method, core fixing glue and steel bands can be eliminated. Also with the machine modification and the small cut, the machine time is also reduced hence the machine cost reduces. Therefore when considering with the conventional cut core method, there is a huge saving on manufacturing cost in the new slotted core method.

CONCLUSION AND SUGGESTIONS FOR FUTURE RESEARCH

6.1 Conclusion

In this research study, it emphasized that the transformer based inrush mitigation methods are more reliable over the external equipment based (i.e. connecting NTC thermistor, start-up resistive load) inrush mitigation methods. Further, this research established the use of slotted cores as the best option over the existing transformer based solutions to mitigate inrush current and several other drawbacks of the conventional solutions.

The proposed method has the advantages of higher performance; lower inrush current, lower no-load current, mechanically stable reinforced structure, easier manufacturing and hence reduced material wastage. So the proposed method saves costs and also the resources. The slotted core is highly reliable on inrush mitigation for the 1kVA transformers, the reduction in inrush current was 40-50% compared to the corresponding conventional transformers.

The main disadvantage of slotted core was the increment of the active core loss, but obviously that has to be sacrificed in order to limit inrush current. But it is still lesser than the loss of the conventional cut core method.

6.2 Suggestions for Future Research

Followings are the future research suggestions, on the slotted core method discussed.

1) This research is confined to particular steel type which is M5 steel grade, and transformer power range. So the same calculation methodology can be used to expand the ranges of above parameters while introducing new steel types.

2) This research has done experiments only for 230V main input. But it will be useful building the same concept for the other common input voltages of other countries / applications (110V, 120V, 200V, 400V etc.), expanding the design calculation.

3) Also there will be more easier and economical manufacturing methods slotted cores; like introducing laser cutting, etc.

   Also it will be worth experimenting for other constructional methods, which could be economical and might be high performing.

REFERENCE LIST

[1] H.K. Ekanayake, “Methodology to limit inrush current of toroidal transformers”, Charted Engineering IESL Sri Lanka, 2012

[2] Rasim Dogan, Saeed Jazebi, ”Investigation of Transformer-Based Solutions for the Reduction of Inrush and Phase-Hop Currents”, IEEE Transactions on Power Electronics, Vol. 31, Iss 5, pp 3506 – 3516, July 2015

[3] Francisco de L, Brian G, “Transformer Based Solutions to Power Quality Problems”, Plitron Manufacturing Inc. Canada, 2001

[4] KAWASAKI STEEL CORPORATION, “PLASMA CORE RGHPJ RGH AND RG CORE”, Grain-Oriented Magnetic Steel Strip, Japan: 1991.

[5] Colonel MW, T. Mclyman, “Transformer and inductor design handbook”, Third Edition, Kg Magnetics, Inc. California, USA, 2004, pp. 96-100

[6] Saeed Jazebi, Nicholas Wu, “Enhanced analytical method for the calculation of the maximum inrush current of single phase power transformer”, IEEE Transactions on Power Delivery, Vol. 30, Iss 6, pp 2590 - 2599, June 2015

[7] Yunfei Wang, Sami G., “Analytical formula to estimate the maximum inrush current”, IEEE Translations on Power Delivery, Vol. 23, No 2, pp 1266 - 1268, April 2008

APPENDICES

Appendix A – Design simulations with ToroidEZE programme with 1.6T to 0.9T flux density

AA-182040 1.6T Design

Core : 180 x 75 x 35 mm 30-M5	Iron Loss : 5.75 W	Finished Dim's : 193 x 45 x 56 mm
Fe Weight : 5.54 kg	Coil Weight : 2.52 kg	Tot. Weight : 8.192 kg
Induction : 1.6 T	Load Loss : 37.35 W	Tot. Power : 1000 VA
Frequency : 50 Hz	Sec Loss : 20.84 W	Temp. Rise : 52/62 deg.C
Excitation: 43.4 mA	Pri Loss : 16.52 W	Optimized : 1:0.88 Wdg+
Core/Coil : 2.2:1 kg	Window Fill : 89.8 %	Wire Fill : 32.2 %

Windings.	Primary	Sec 1
	0	0
Rated Volts rms.	230v	230v
Rated Amps rms.	4.54A	4.35A
Duty Cycle %.	-	100%
	-	-
VA rms.	-	1000
Conductor.	Cu	Cu
Turns.	371ts	384ts
Wire Gauge.	1.600mm	1.500mm
Filars.	-	-
	-	-
Ohms @ 20°C.	0.592	0.812
	-	-
Winding grams.	1222	1294
	-	-
Full-Load Volts.	-	230.1v
No-Load Volts.	-	238.1v
Regulation %.	1.5%	3.3%
	-	-
Watts Loss Hot.	16.52	20.84
	-	-
Insulation Tape.	-	-
Width. mm.	13	-
Thickness. mm.	0.1	-
Layers.	4	-
	-	-
Screening Tape.	-	-
Width. mm.	-	-
Thickness. mm.	-	-
Layers.	-	-
	-	-
A/mm^2.	2.26	2.46
Bare Wire Fill %	16.89%	15.36%

ToroidEZE-AL v.2.6.4 Page 1 of 1.

AA-182040 1.5T Design

Design File : ED 1kva - 1.5.tfx

Core :	180 x 75 x 35 mm 30-M5	Iron Loss	: 4.86 W	Finished Dim's	: 194 x 44 x 57 mm
Fe Weight :	5.54 kg	Coil Weight	: 2.69 kg	Tot. Weight	: 8.366 kg
Induction :	1.499 T	Load Loss	: 40.15 W	Tot. Power	: 1000 VA
Frequency :	50 Hz	Sec Loss	: 22.44 W	Temp. Rise	: 53/63 deg.C
Excitation:	33.4 mA	Pri Loss	: 17.71 W	Optimized	: 1:0.82 Wdg+
Core/Coil :	2.1:1 kg	Window Fill	: 93.1 %	Wire Fill	: 34.5 %

Windings.	Primary	Sec 1
	0	0
Rated Volts rms.	230v	230v
Rated Amps rms.	4.54A	4.35A
Duty Cycle %.	-	100%
	-	-
VA rms.	-	1000
Conductor.	Cu	Cu
Turns.	396ts	411ts
Wire Gauge.	1.600mm	1.500mm
Filars.	-	-
	-	-
Ohms @ 20°C.	0.63	0.871
	-	-
Winding grams.	1301	1388
	-	-
Full-Load Volts.	-	230.2v
No-Load Volts.	-	238.7v
Regulation %.	1.6%	3.6%
	-	-
Watts Loss Hot.	17.71	22.44
	-	-
Insulation Tape.	-	-
Width. mm.	13	-
Thickness. mm.	0.1	-
Layers.	4	-
	-	-
Screening Tape.	-	-
Width. mm.	-	-
Thickness. mm.	-	-
Layers.	-	-
	-	-
A/mm^2.	2.26	2.46
Bare Wire Fill %	18.02%	16.44%

ToroidEZE-AL v.2.6.4 *Page 1 of 1.*

AA-182040 1.4T Design

Design File : ED 1kva - 1.4.tfx

Core : 180 x 75 x 35 mm 30-M5	Iron Loss : 4.18 W	Finished Dim's : 194 x 42 x 58 mm
Fe Weight : 5.54 kg	Coil Weight : 2.93 kg	Tot. Weight : 8.607 kg
Induction : 1.4 T	Load Loss : 44.22 W	Tot. Power : 1000 VA
Frequency : 50 Hz	Sec Loss : 24.67 W	Temp. Rise : 55/66 deg.C
Excitation: 27.3 mA	Pri Loss : 19.55 W	Optimized : 1:0.76 Wdg+
Core/Coil : 1.9:1 kg	Window Fill : 96.7 %	Wire Fill : 37 %

Windings.	Primary	Sec 1
	0	0
Rated Volts rms.	230v	230v
Rated Amps rms.	4.56A	4.35A
Duty Cycle %.	-	100%
	-	-
VA rms.	-	1000
Conductor.	Cu	Cu
Turns.	424ts	442ts
Wire Gauge.	1.600mm	1.500mm
Filars.	-	-
	-	-
Ohms @ 20°C.	0.686	0.95
	-	-
Winding grams.	1415	1514
	-	-
Full-Load Volts.	-	230.4v
No-Load Volts.	-	239.8v
Regulation %.	1.8%	3.9%
	-	-
Watts Loss Hot.	19.55	24.67
	-	-
Insulation Tape.	-	-
Width. mm.	13	-
Thickness. mm.	0.1	-
Layers.	4	-
	-	-
Screening Tape.	-	-
Width. mm.	-	-
Thickness. mm.	-	-
Layers.	-	-
	-	-
A/mm^2.	2.27	2.46
Bare Wire Fill %	19.3%	17.68%

ToroidEZE-AL v.2.6.4 *Page 1 of 1.*

AA-182040 1.3T Design

Design File : ED 1kva - 1.3.tfx

Core	: 180 x 75 x 35 mm 30-M5	Iron Loss	: 3.59 W	Finished Dim's	: 195 x 40 x 59 mm
Fe Weight	: 5.54 kg	Coil Weight	: 3.19 kg	Tot. Weight	: 8.874 kg
Induction	: 1.299 T	Load Loss	: 48.86 W	Tot. Power	: 1000 VA
Frequency	: 50 Hz	Sec Loss	: 27.49 W	Temp. Rise	: 58/70 deg.C
Excitation	: 23 mA	Pri Loss	: 21.37 W	Optimized	: 1:0.69 Wdg+
Core/Coil	: 1.7:1 kg	Window Fill	: 100.8 %	Wire Fill	: 39.9 %

Windings.	Primary	Sec 1
	0	0
Rated Volts rms.	230v	230v
Rated Amps rms.	4.58A	4.35A
Duty Cycle %.	-	100%
	-	-
VA rms.	-	1000
Conductor.	Cu	Cu
Turns.	457ts	478ts
Wire Gauge.	1.600mm	1.500mm
Filars.	-	-
	-	-
Ohms @ 20°C.	0.738	1.05
	-	-
Winding grams.	1522	1672
	-	-
Full-Load Volts.	-	230.2v
No-Load Volts.	-	240.6v
Regulation %.	1.9%	4.3%
	-	-
Watts Loss Hot.	21.37	27.49
	-	-
Insulation Tape.	-	-
Width. mm.	13	-
Thickness. mm.	0.1	-
Layers.	4	-
	-	-
Screening Tape.	-	-
Width. mm.	-	-
Thickness. mm.	-	-
Layers.	-	-
	-	-
A/mm^2.	2.28	2.46
Bare Wire Fill %	20.8%	19.12%

ToroidEZE-AL v.2.6.4 *Page 1 of 1.*

AA-182040 1.2T Design

Design File : ED 1kva - 1.2.tfx

Core :	180 x 75 x 35 mm 30-M5	Iron Loss	: 3.09 W	Finished Dim's	: 196 x 38 x 61 mm
Fe Weight :	5.54 kg	Coil Weight	: 3.47 kg	Tot. Weight	: 9.15 kg
Induction :	1.199 T	Load Loss	: 53.64 W	Tot. Power	: 1000 VA
Frequency :	50 Hz	Sec Loss	: 30.02 W	Temp. Rise	: 61/73 deg.C
Excitation:	19.6 mA	Pri Loss	: 23.62 W	Optimized	: 1:0.64 Wdg+
Core/Coil :	1.6:1 kg	Window Fill	: 105.4 %	Wire Fill	: 43.3 %

Windings.	Primary	Sec 1
	0	0
Rated Volts rms.	230v	230v
Rated Amps rms.	4.59A	4.35A
Duty Cycle %.	-	100%
	-	-
VA rms.	-	1000
Conductor.	Cu	Cu
Turns.	495ts	520ts
Wire Gauge.	1.600mm	1.500mm
Filars.	-	-
	-	-
Ohms @ 20°C.	0.802	1.14
	-	-
Winding grams.	1656	1812
	-	-
Full-Load Volts.	-	230.3v
No-Load Volts.	-	241.6v
Regulation %.	2.1%	4.7%
	-	-
Watts Loss Hot.	23.62	30.02
	-	-
Insulation Tape.	-	-
Width. mm.	13	-
Thickness. mm.	0.1	-
Layers.	4	-
	-	-
Screening Tape.	-	-
Width. mm.	-	-
Thickness. mm.	-	-
Layers.	-	-
	-	-
A/mm^2.	2.29	2.46
Bare Wire Fill %	22.53%	20.8%

ToroidEZE-AL v.2.6.4 *Page 1 of 1.*

AA-182040 1.1T Design

Design File : ED 1kva - 1.1.tfx

Core	: 180 x 75 x 35 mm 30-M5	Iron Loss	: 2.64 W	Finished Dim's	: 197 x 35 x 63 mm
Fe Weight	: 5.54 kg	Coil Weight	: 3.88 kg	Tot. Weight	: 9.561 kg
Induction	: 1.099 T	Load Loss	: 61.31 W	Tot. Power	: 1000 VA
Frequency	: 50 Hz	Sec Loss	: 34.47 W	Temp. Rise	: 66/79 deg.C
Excitation	: 16.6 mA	Pri Loss	: 26.84 W	Optimized	: 1:0.57 Wdg+
Core/Coil	: 1.4:1 kg	Window Fill	: 110.7 %	Wire Fill	: 47.4 %

Windings.	Primary	Sec 1
	0	0
Rated Volts rms.	230v	230v
Rated Amps rms.	4.63A	4.35A
Duty Cycle %.	-	100%
	-	-
VA rms.	-	1000
Conductor.	Cu	Cu
Turns.	540ts	571ts
Wire Gauge.	1.600mm	1.500mm
Filars.	-	-
	-	-
Ohms @ 20°C.	0.887	1.29
	-	-
Winding grams.	1828	2049
	-	-
Full-Load Volts.	-	230.3v
No-Load Volts.	-	243.2v
Regulation %.	2.4%	5.3%
	-	-
Watts Loss Hot.	26.84	34.47
	-	-
Insulation Tape.	-	-
Width. mm.	13	-
Thickness. mm.	0.1	-
Layers.	4	-
	-	-
Screening Tape.	-	-
Width. mm.	-	-
Thickness. mm.	-	-
Layers.	-	-
	-	-
A/mm^2.	2.3	2.46
Bare Wire Fill %	24.59%	22.84%

ToroidEZE-AL v.2.6.4 *Page 1 of 1.*

AA-182040 1.0T Design

Design File : ED 1kva - 1.0.tfx

Core : 180 x 75 x 35 mm 30-M5	Iron Loss : 2.24 W	Finished Dim's : 195 x 38 x 61 mm
Fe Weight : 5.54 kg	Coil Weight : 3.41 kg	Tot. Weight : 9.09 kg
Induction : 0.999 T	Load Loss : 74.69 W	Tot. Power : 1000 VA
Frequency : 50 Hz	Sec Loss : 40.47 W	Temp. Rise : 79/94 deg.C
Excitation: 13.9 mA	Pri Loss : 34.21 W	Optimized : 1:0.65 Wdg+
Core/Coil : 1.6:1 kg	Window Fill : 104.7 %	Wire Fill : 41.4 %

Windings.	Primary	Sec 1
	0	0
Rated Volts rms.	230v	230v
Rated Amps rms.	4.52A	4.35A
Duty Cycle %.	-	100%
	-	-
VA rms.	-	1000
Conductor.	Cu	Cu
Turns.	594ts	636ts
Wire Gauge.	1.400mm	1.400mm
Pilars.	-	-
	-	-
Ohms @ 20°C.	1.24	1.58
	-	-
Winding grams.	1499	1911
	-	-
Full-Load Volts.	-	230.3v
No-Load Volts.	-	246.3v
Regulation %.	3.1%	6.5%
	-	-
Watts Loss Hot.	34.21	40.47
	-	-
Insulation Tape.	-	-
Width. mm.	13	-
Thickness. mm.	0.1	-
Layers.	4	-
	-	-
Screening Tape.	-	-
Width. mm.	-	-
Thickness. mm.	-	-
Layers.	-	-
	-	-
A/mm^2.	2.94	2.83
Bare Wire Fill %	20.7%	20.7%

ToroidEZE-AL v.2.6.4 *Page 1 of 1.*

AA-182040 0.9T Design

Design File : ED 1kva - 0.9.tfx

Core : 180 x 75 x 35 mm 30-M5	Iron Loss : 1.84 W	Finished Dim's : 197 x 35 x 63 mm
Fe Weight : 5.54 kg	Coil Weight : 3.92 kg	Tot. Weight : 9.602 kg
Induction : 0.899 T	Load Loss : 104.9 W	Tot. Power : 1000 VA
Frequency : 50 Hz	Sec Loss : 54.42 W	Temp. Rise : 100/120 deg.C
Excitation: 11.5 mA	Pri Loss : 50.48 W	Optimized : 1:0.57 Wdg+
Core/Coil : 1.4:1 kg	Window Fill : 111.6 %	Wire Fill : 48.2 %

Windings.	Primary	Sec 1
	0	0
Rated Volts rms.	230v	230v
Rated Amps rms.	4.81A	4.35A
Duty Cycle %.	-	100%
	-	-
VA rms.	-	1000
Conductor.	Cu	Cu
Turns.	660ts	724ts
Wire Gauge.	1.400mm	1.400mm
Filars.	-	-
	-	-
Ohms @ 20°C.	1.4	1.85
	-	-
Winding grams.	1692	2228
	-	-
Full-Load Volts.	-	230.6v
No-Load Volts.	-	252.3v
Regulation %.	4.3%	8.6%
	-	-
Watts Loss Hot.	50.48	54.42
	-	-
Insulation Tape.	-	-
Width. mm.	13	-
Thickness. mm.	0.1	-
Layers.	4	-
	-	-
Screening Tape.	-	-
Width. mm.	-	-
Thickness. mm.	-	-
Layers.	-	-
	-	-
A/mm^2.	3.13	2.83
Bare Wire Fill %	23%	25.23%

ToroidEZE-AL v.2.6.4 *Page 1 of 1.*

Appendix B – Test equipment details

Mixed Signal Oscilloscope (DPO3000)

Mixed Signal Oscilloscopes

MSO3000 Series, DPO3000 Series Data Sheet

Features & Benefits

Key Performance Specifications

- 500, 300, 100 MHz Bandwidth Models
- 2 and 4 Analog Channel Models
- 16 Digital Channels (MSO Series)
- 2.5 GS/s Sample Rate on All Channels
- 5 Megapoint Record Length on All Channels
- >50,000 wfm/s Maximum Waveform Capture Rate
- Suite of Advanced Triggers

Ease of Use Features

- Wave Inspector® Controls provide Easy Navigation and Automated Search of Waveform Data
- 29 Automated Measurements, and FFT Analysis for Simplified Waveform Analysis
- TekVPI® Probe Interface Supports Active, Differential, and Current Probes for Automatic Scaling and Units
- 9 in. (229 mm) WVGA Widescreen Color Display
- Small Footprint and Lightweight – Only 5.8 in. (147 mm) deep and 9 lb. (4 kg)

Connectivity

- USB 2.0 Host Port on both the Front Panel and Rear Panel for Quick and Easy Data Storage, Printing, and Connecting a USB Keyboard
- USB 2.0 Device Port on Rear Panel for Easy Connection to a PC or Direct Printing to a PictBridge®-compatible Printer
- Integrated 10/100 Ethernet Port for Network Connection and Video Out Port to Export the Oscilloscope Display to a Monitor or Projector

Optional Serial Triggering and Analysis

- Automated Serial Triggering, Decode, and Search Options for I²C, SPI, CAN, LIN, RS-232/422/485/UART, and I²S/LJ/RJ/TDM

Mixed Signal Design and Analysis (MSO Series)

- Automated Triggering, Decode, and Search on Parallel Buses
- Multichannel Setup and Hold Triggering
- MagniVu™ High-speed Acquisition Provides 121.2 ps Fine Timing Resolution on Digital Channels

Optional Application Support

- Power Analysis
- HDTV and Custom Video Analysis

Feature-rich Tools for Debugging Mixed Signal Designs

With the MSO/DPO3000 Mixed Signal Oscilloscope Series, you can analyze up to 20 analog and digital signals with a single instrument to quickly find and diagnose problems in complex designs. Bandwidths up to 500 MHz and a minimum of 5X oversampling on all channels ensure you have the performance you need for many of today's mainstream applications. To capture long windows of signal activity while maintaining fine timing resolution, the MSO/DPO3000 offers a deep record length of 5 Mpoints standard on all channels.

With Wave Inspector® controls for rapid waveform navigation, automated serial and parallel bus analysis, and automated power analysis – the MSO/DPO3000 Oscilloscope Series from Tektronix provides the feature-rich tools you need to simplify and speed debug of your complex design.

Tektronix®

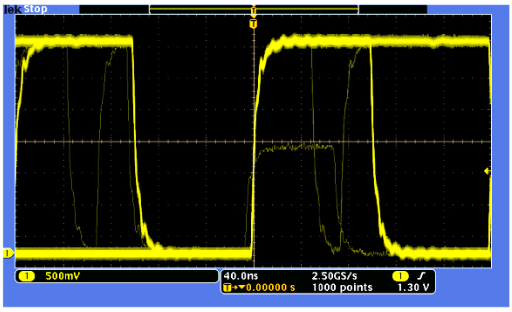

Discover – Fast waveform capture rate - over 50,000 wfm/s - maximizes the probability of capturing elusive glitches and other infrequent events.

Comprehensive Features Speed Every Stage of Debug

The MSO/DPO3000 Series offers a robust set of features to speed every stage of debugging your design – from quickly discovering an anomaly and capturing it, to searching your waveform record for the event and analyzing its characteristics and your device's behavior.

Discover

To debug a design problem, first you must know it exists. Every design engineer spends time looking for problems in their design, a time-consuming and frustrating task without the right debug tools.

The MSO/DPO3000 Series offers the industry's most complete visualization of signals, providing fast insight into the real operation of your device. A fast waveform capture rate – greater than 50,000 waveforms per second – enables you to see glitches and other infrequent transients within seconds, revealing the true nature of device faults. A digital phosphor display with intensity grading shows the history of a signal's activity by intensifying areas of the signal that occur more frequently, providing a visual display of just how often anomalies occur.

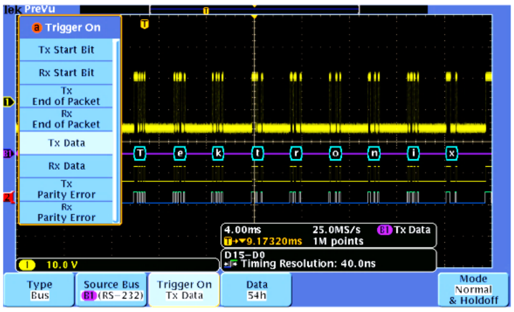

Capture – Triggering on a specific transmit data packet going across an RS-232 bus. A complete set of triggers, including triggers for specific serial packet content, ensures you quickly capture your event of interest.

Capture

Discovering a device fault is only the first step. Next, you must capture the event of interest to identify root cause.

The MSO/DPO3000 Series provides a complete set of triggers – including runt, logic, pulse width/glitch, setup/hold violation, serial packet, and parallel data – to help quickly find your event. With up to a 5 Mpoint record length, you can capture many events of interest, even thousands of serial packets, in a single acquisition for further analysis while maintaining high resolution to zoom in on fine signal details.

From triggering on specific packet content to automatic decode in multiple data formats, the MSO/DPO3000 Series provides integrated support for the industry's broadest range of serial buses – I²C, SPI, CAN, LIN, RS-232/422/485/UART, and I²S/LJ/RJ/TDM. The ability to decode up to two serial and/or parallel buses simultaneously means you gain insight into system-level problems quickly.

To further help troubleshoot system-level interactions in complex embedded systems, the MSO3000 Series offers 16 digital channels in addition to its analog channels. Since the digital channels are fully integrated into the oscilloscope, you can trigger across all input channels, automatically time-correlating all analog, digital, and serial signals. The MagniVu™ high-speed acquisition enables you to acquire fine signal detail (up to 121.2 ps resolution) around the trigger point for precision measurements. MagniVu is essential for making accurate timing measurements for setup and hold measurements, clock delay, signal skew, and glitch characterization.

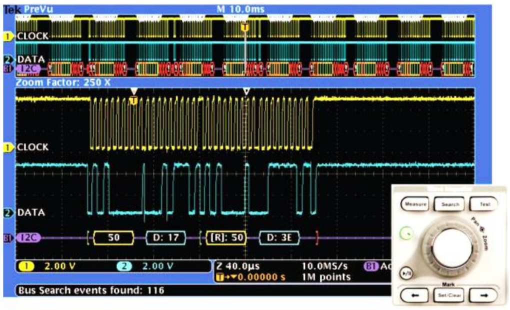

Search – I²C decode showing results from a Wave Inspector search for Address value 50. Wave Inspector controls provide unprecedented efficiency in viewing and navigating waveform data.

Search

Finding your event of interest in a long waveform record can be time consuming without the right search tools. With today's record lengths pushing beyond a million data points, locating your event can mean scrolling through thousands of screens of signal activity.

The MSO/DPO3000 Series offers the industry's most comprehensive search and waveform navigation with its innovative Wave Inspector® controls. These controls speed panning and zooming through your record. With a unique force-feedback system, you can move from one end of your record to the other in just seconds. User marks allow you to mark any location that you may want to reference later for further investigation. Or, automatically search your record for criteria you define. Wave Inspector will instantly search your entire record, including analog, digital, and serial bus data. Along the way it will automatically mark every occurrence of your defined event so you can quickly move between events.

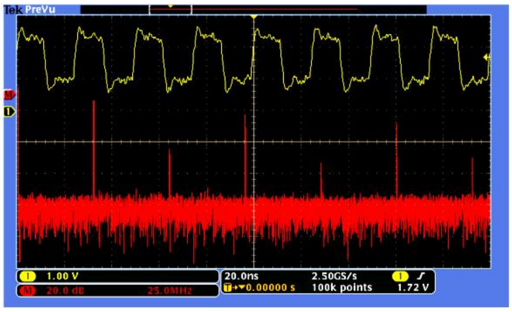

Analyze – FFT analysis of a pulsed signal. A comprehensive set of integrated analysis tools speeds verification of your design's performance.

Analyze

Verifying that your prototype's performance matches simulations and meets the project's design goals requires analyzing its behavior. Tasks can range from simple checks of rise times and pulse widths to sophisticated power loss analysis and investigation of noise sources.

The MSO/DPO3000 Series offers a comprehensive set of integrated analysis tools including waveform- and screen-based cursors, 29 automated measurements, advanced waveform math including arbitrary equation editing, FFT analysis, and trend plots for visually determining how a measurement is changing over time. Specialized application support for serial bus analysis, power supply design, and video design and development is also available.

For extended analysis, National Instrument's LabVIEW SignalExpress™ Tektronix Edition provides over 200 built-in functions including time and frequency domain analysis, limit testing, data logging, and customizable reports.

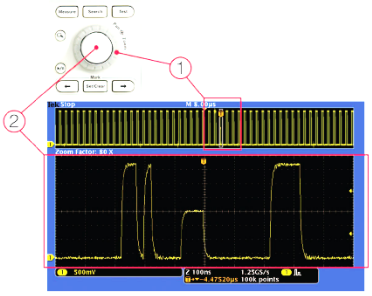

Wave Inspector controls provide unprecedented efficiency in viewing, navigating, and analyzing waveform data. Zip through your 5 Mpoint record by turning the outer pan control (1). Get from the beginning to end in seconds. See something of interest and want to see more details? Just turn the inner zoom control (2).

Wave Inspector® Navigation and Search

A 5 Mpoint record length represents thousands of screens of information. The MSO/DPO3000 Series enables you to find your event in seconds with Wave Inspector, the industry's best tool for navigation and search.

Wave Inspector offers the following innovative controls:

Zoom/Pan

A dedicated, two-tier front-panel control provides intuitive control of both zooming and panning. The inner control adjusts the zoom factor (or zoom scale); turning it clockwise activates zoom and goes to progressively higher zoom factors, while turning it counterclockwise results in lower zoom factors and eventually turning zoom off. No longer do you need to navigate through multiple menus to adjust your zoom view. The outer control pans the zoom box across the waveform to quickly get to the portion of waveform you are interested in. The outer control also utilizes force-feedback to determine how fast to pan on the waveform. The farther you turn the outer control, the faster the zoom box moves. Pan direction is changed by simply turning the control the other way.

Play/Pause

A dedicated **Play/Pause** front-panel button scrolls the waveform across the display automatically while you look for anomalies or an event of interest. Playback speed and direction are controlled using the intuitive pan control. Once again, turning the control further makes the waveform scroll faster and changing direction is as simple as turning the control the other way.

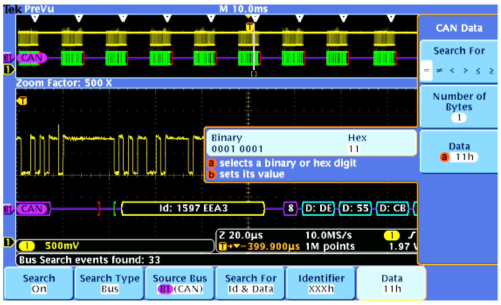

Search step 1: You define what you would like to find.

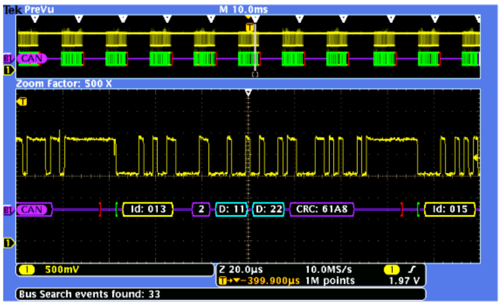

Search step 2: Wave Inspector automatically searches through the record and marks each event with a hollow white triangle. You can then use the **Previous** and **Next** buttons to jump from one event to the next.

User Marks

Press the **Set Mark** front-panel button to place one or more marks on the waveform. Navigating between marks is as simple as pressing the **Previous** (←) and **Next** (→) buttons on the front panel.

Search Marks

The **Search** button allows you to automatically search through your long acquisition looking for user-defined events. All occurrences of the event are highlighted with search marks and are easily navigated to, using the front-panel **Previous** (←) and **Next** (→) buttons. Search types include edge, pulse width/glitch, runt, logic, setup and hold, rise/fall time parallel bus, and I²C, SPI, CAN, LIN, RS-232/422/485/UART, and I²S/LJ/RJ/TDM packet content.

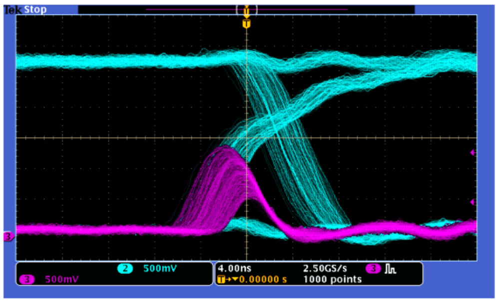

Digital phosphor technology enables greater than 50,000 wfm/s waveform capture rate and real-time intensity grading on the MSO/DPO3000 Series.

Digital Phosphor Technology

The MSO/DPO3000 Series' digital phosphor technology provides you with fast insight into the real operation of your device. Its fast waveform capture rate – greater than 50,000 wfm/s – gives you a high probability of quickly seeing the infrequent problems common in digital systems: runt pulses, glitches, timing issues, and more.

Waveforms are superimposed with one another and waveform points that occur more frequently are intensified. This quickly highlights the events that over time occur more often or, in the case of infrequent anomalies, occur less often.

With the MSO/DPO3000 Series, you can choose infinite persistence or variable persistence, determining how long the previous waveform acquisitions stay on-screen. This allows you to determine how often an anomaly is occurring.

Mixed Signal Design and Analysis (MSO Series)

The MSO3000 Series Mixed Signal Oscilloscopes provide 16 digital channels. These channels are tightly integrated into the oscilloscope's user interface, simplifying operation and making it possible to solve mixed-signal issues easily.

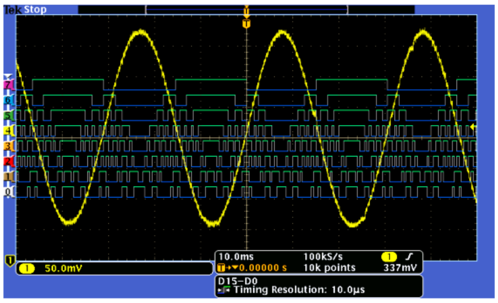

The MSO Series provides 16 integrated digital channels enabling you to view and analyze time-correlated analog and digital signals.

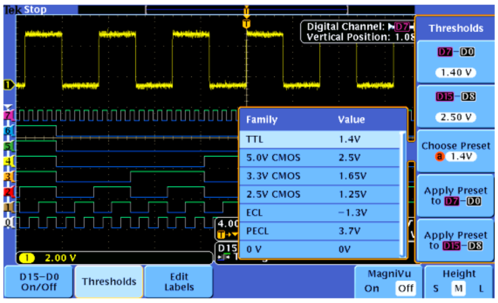

With the color-coded digital waveform display, groups are created by simply placing digital channels together on the screen, allowing the digital channels to be moved as a group. You can set threshold values for each pod of eight channels, enabling support for up to two different logic families.

Color-coded Digital Waveform Display

The MSO3000 Series has redefined the way you view digital waveforms. One common problem shared by both logic analyzers and mixed-signal oscilloscopes is determining if data is a one or a zero when zoomed in far enough that the digital trace stays flat all the way across the display. The MSO3000 Series has color-coded digital traces, displaying ones in green and zeros in blue.

Characteristics

Vertical System Analog Channels

Characteristic	MSO3012 DPO3012	MSO3014 DPO3014	MSO3032 DPO3032	MSO3034 DPO3034	DPO3052	MSO3054 DPO3054
Input Channels	2	4	2	4	2	4
Analog Bandwidth (–3 dB)	100 MHz	100 MHz	300 MHz	300 MHz	500 MHz	500 MHz
Calculated Rise Time 5 mV/div (typical)	3.5 ns	3.5 ns	1.17 ns	1.17 ns	700 ps	700 ps
Hardware Bandwidth Limits	20 MHz		20 MHz, 150 MHz			
Input Coupling	AC, DC, GND					
Input Impedance	1 MΩ ±1%, 75 Ω ±1%, 50 Ω ±1%					
Input Sensitivity Range, 1 MΩ	1 mV/div to 10 V/div					
Input Sensitivity Range, 75 Ω, 50 Ω	1 mV/div to 1 V/div					
Vertical Resolution	8 bits (11 bits with Hi Res)					
Maximum Input Voltage, 1 MΩ	300 V_{RMS} with peaks ≤ ±450 V					
Maximum Input Voltage, 75 Ω, 50 Ω	5 V_{RMS} with peaks ≤ ±20 V					
DC Gain Accuracy	±1.5% for 5 mV/div and above ±2.0% for 2 mV/div ±2.5% for 1 mV/div					
Channel-to-Channel Isolation (Any Two Channels at Equal Vertical Scale)	≥100:1 at ≤100 MHz and ≥30:1 at >100 MHz up to the rated BW					

Offset Range

Range	1 MΩ	50 Ω, 75 Ω
1 mV/div to 99.5 mV/div	±1 V	±1 V
100 mV/div to 995 mV/div	±10 V	±5 V
1 V/div	±100 V	±5 V
1.01 V/div to 10 V/div	±100 V	NA

Vertical System Digital Channels

Characteristic	All MSO3000 Models
Input Channels	16 Digital (D15 to D0)
Thresholds	Threshold per set of 8 channels
Threshold Selections	TTL, CMOS, ECL, PECL, User Defined
User-defined Threshold Range	–15 V to +25 V
Maximum Input Voltage	–20 V to +30 V
Threshold Accuracy	±(100 mV +3% of threshold setting)
Maximum Input Dynamic Range	50 V_{p-p} (threshold setting dependent)
Minimum Voltage Swing	500 mV_{p-p}
Input Impedance	101 kΩ
Probe Loading	8 pF
Vertical Resolution	1 bit

Horizontal System Analog Channels

Characteristic	All MSO3000 Models All DPO3000 Models
Maximum Sample Rate (all channels)	2.5 GS/s
Maximum Record Length (all channels)	5 Mpoints
Maximum Duration of Time Captured at Highest Sample Rate (all channels)	2 ms
Time-base Range (s/div)	1 ns to 1000 s
Time-base Delay Time Range	–10 divisions to 5000 s
Channel-to-Channel Deskew Range	±100 ns
Time-base Accuracy	±10 ppm over any ≥1 ms interval

Horizontal System Digital Channels

Characteristic	All MSO3000 Models
Maximum Sample Rate (Main, all channels)	500 MS/s (2 ns resolution)
Maximum Record Length (Main, all channels)	5 Mpoints
Maximum Sample Rate (MagniVu, all channels)	8.25 GS/s (121.2 ps resolution)
Maximum Record Length (MagniVu, all channels)	10 kpoints centered on the trigger
Minimum Detectable Pulse Width	2.0 ns
Channel-to-Channel Skew	500 ps typical

Current Probes (DPO3000)

Tektronix

Current Probes

A621 & A622 Datasheet

DS_FeaturesBenefitsContainer

The A600 Series current probes are specifically designed to support measurements with the TekMeter® or oscilloscope.

Features and benefits

- A621
  - AC – 5 Hz to 50 kHz
  - 100 mA to 2000 A peak
  - For DMMs and oscilloscopes
  - Clamp on
- A622
  - AC/DC – 100 kHz
  - 50 mA to 100 A peak
  - For DMMs and oscilloscopes

Applications

- Motor drives
- Inverters
- Power supplies
- Avionics

A621 2000 Amp AC Current probe/BNC

This industrial-style clamp-on probe has a BNC connector and can be used with a shrouded banana plug adapter [1] so it can be used on digital multimeters, TekMeter, and oscilloscopes. The A621 can measure AC currents from 100 mA to 2000 A peak over a frequency range of 5 Hz to 50 kHz. It provides a 1 mV, 10 mV, or 100 mV output for each Amp measured.

A622 100 Amp AC DC Current probe/BNC

This "long nose" style clamp-on probe uses a Hall Effect current sensor to provide a voltage output to oscilloscopes. It has a BNC connector and can be used with a shrouded banana plug adapter [1] so it can also be used on digital multimeters, TekMeter, and oscilloscopes. The A622 can measure AC/DC currents from 50 mA to 100 A peak over a frequency range of DC to 100 kHz. It provides 10 mV or 100 mV output for each Amp measured.

Recommended products

TPS2000, TDS1000B, TDS2000C, and TDS3000C Series oscilloscopes and DMM4020 [1], DMM4040 [1], and DMM4050 [1] digital multimeters.

1 For instruments with banana jack inputs, Tektronix part number 012-1450-00 Female BNC to banana lead adapter is required.

Specifications

All specifications are guaranteed unless noted otherwise. All specifications apply to all models unless noted otherwise.

Characteristic	A621	A622
Frequency range	5 Hz to 50 kHz	DC to 100 kHz
Maximum input current	2000 A peak	100 A peak
Output	1 mV/A, 10 mV/A, 100 mV/A	10 mV/A, 100 mV/A
Maximum conductor diameter	54 mm (2.13 in.)	11.8 mm (0.46 in.)
Termination	BNC [1]	BNC [1]
Maximum bare-wire voltage	600 V (CAT III)	600 V (CAT III)
Safety	UL3111-2-032, CSA1010.2.032, EN61010-2-032, IEC61010-2-032	UL3111-2-032, CSA1010.2.032, EN61010-2-032, IEC61010-2-032

Ordering information

A621 2000 A AC Current probe/BNC.

A622 100 A AC/DC Current probe/BNC.

Recommended accessories

012-1450-xx Adapter, lead; discrete – MLD, 2, 18 AWG, dual insul, BNC, female X 4 mm dual insul; banana jack X dual insul plug, shield banana

Options

Service options

Opt. R3 Repair Service 3 Years (including warranty)

Opt. R5 Repair Service 5 Years (including warranty)

Zero crossing detecting circuit (SIEMENS 3RF2050-1AA02)

SIEMENS

Product data sheet **3RF2050-1AA02**

SEMICOND. RELAY 3RF2,
1-PHASE WIDTH 45 MM,
50 A 24-230 V / 24 V DC SCREW TERMINAL

General technical data:		
product brand name		SIRIUS
product designation		solid-state relay
Product function		zero-point switching
Number of poles / for main current circuit		1
Protection class IP		IP20
Ambient temperature		
• during operating	°C	-25 … +60
• during storage	°C	-55 … +80
Installation altitude / at a height over sea level / maximum	m	1,000
Resistance against vibration / according to IEC 60068-2-6		2g
Resistance against shock / according to IEC 60068-2-27		15g / 11 ms
Item designation		
• according to DIN 40719 extendable after IEC 204-2 / according to IEC 750		K
• according to DIN EN 61346-2		Q
Number of NC contacts / for auxiliary contacts		0
Number of NO contacts / for auxiliary contacts		0
Number of change-over switches / for auxiliary contacts		0

Main circuit:

3RF2050-1AA02
Page 1/5
03/06/2013
subject to modifications

Number of NO contacts / for main contacts		1
Number of NC contacts / for main contacts		0
Operating current		
• at AC-1 / at 400 V / rated value	A	50
• at AC-51 / rated value	A	50
Operating current / minimum	mA	500
Operating voltage		
• at 50 Hz / at AC / rated value	V	24 … 230
• at 60 Hz / at AC / rated value	V	24 … 230
Working area related to the operating voltage		
• at 50 Hz / for AC	V	20 … 253
• at 60 Hz / for AC	V	20 … 253
Operating frequency		
• rated value	Hz	50 … 60
Relative symmetrical tolerance / of the operation frequency	%	10
Insulation voltage / rated value	V	600
Voltage slew rate / at the thyristor / for main contacts / maximum permissible	V/µs	1,000
Block voltage / at the thyristor / for main contacts / maximum permissible	V	800
Reverse current / of the thyristor	mA	10
Derating temperature	°C	40
Active power loss / total / typical	W	66
Resistance against the impulse current / rated value	A	600
I2t-level / maximum	$A^2 \cdot s$	1,800

Control circuit:		
Type of voltage / of the controlled supply voltage		DC
Control supply voltage / 1		
• for DC		
• initial rated value	V	15
• final rated value	V	24
Control supply voltage		
• for DC / final value for signal<0>-recognition	V	5
Relative symmetrical tolerance / of the supply voltage frequency	%	10
Control current		
• at minimum control supply voltage / for DC	mA	2
• for DC / rated value	mA	15
Fuse assignments		https://www.automation.siemens.com/cd-static/material/info/3RF20_eng.pdf

Installation/mounting/dimensions:		
Type of mounting		screw fixing
Type of fixing/fixation / series installation		Yes
Design of the thread / of the screw for fastening of the operating resource		M4
Tightening torque / of the screw for fastening of the operating resource	N·m	1.5
Width	mm	45
Height	mm	58
Depth	mm	48

Connections:		
Design of the electrical connection / for main current circuit		screw-type terminals
Design of the thread / of the connection screw / for main contacts		M4
Tightening torque / for main contacts / with screw-type terminals		
• minimum	N·m	2
• maximum	N·m	2.5
Tightening torque (lbf·in) / for main contacts / with screw-type terminals		
• minimum	lbf·in	7
• maximum	lbf·in	10.3
Type of the connectable conductor cross-section		
• for main contacts		
• solid		2x (1.5 ... 2.5 mm²), 2x (2.5 ... 6 mm²)
• finely stranded		
• with conductor end processing		2x (1 ... 2.5 mm²), 2x (2.5 ... 6 mm²), 1x 10 mm²
• for AWG conductors		
• for main contacts		2x (14 ... 10)
• for auxiliary and control contacts		1x (AWG 20 ... 12)
• for auxiliary and control contacts		
• solid		1x (0.5 ... 2.5 mm²), 2x (0.5 ... 1.0 mm²)
• finely stranded		
• with conductor end processing		1x (0.5 ... 2.5 mm²), 2x (0.5 ... 1.0 mm²)
• without conductor final cutting		1x (0.5 ... 2.5 mm²), 2x (0.5 ... 1.0 mm²)
Conductor cross section that can be connected		
• for main contacts		
• solid	mm²	1.5 … 6
• stranded wire		
• with conductor end processing	mm²	1 … 10
• for auxiliary and control contacts		

• solid	mm²	0.5 … 2.5
• stranded wire		
• with conductor end processing /	mm²	0.5 … 2.5
• without conductor final cutting	mm²	0.5 … 2.5
AWG number / as coded connectable conductor cross-section / for main contacts		14 … 10
Design of the electrical connection / for auxiliary and control current circuit		screw-type terminals
Design of the thread / of the connection screw / of the auxiliary and control pins		M3
AWG number / as coded connectable conductor cross-section		
• for auxiliary and control contacts		20 … 12
Skinning length / of the cable / for main contacts	mm	10
Skinning length / of the cable / for auxiliary and control contacts	mm	7
Tightening torque / for auxiliary and control contacts		
• with screw-type terminals	N·m	0.5 … 0.6
Tightening torque (lbf·in) / for auxiliary and control contacts		
• with screw-type terminals	lbf·in	4.5 … 5.3

Certificates/approvals:

General Product Approval			EMC	Declaration of Conformity	Test Certificates
CSA	GOST	UR	C-TICK	EG-Konf.	Type Test Certificates/Test Report

other

Environmental Confirmations

Further information:

Information- and Downloadcenter (Catalogs, Brochures,…)
http://www.siemens.com/industrial-controls/catalogs

Industry Mall (Online ordering system)
http://www.siemens.com/industrial-controls/mall

CAx-Online-Generator
http://www.siemens.com/cax

Service&Support (Manuals, Certificates, Characteristics, FAQs,...)
http://support.automation.siemens.com/WW/view/en/3RF2050-1AA02/all

Image database (product images, 2D dimension drawings, 3D models, device circuit diagrams, ...)
http://www.automation.siemens.com/bilddb/cax_en.aspx?mlfb=3RF2050-1AA02

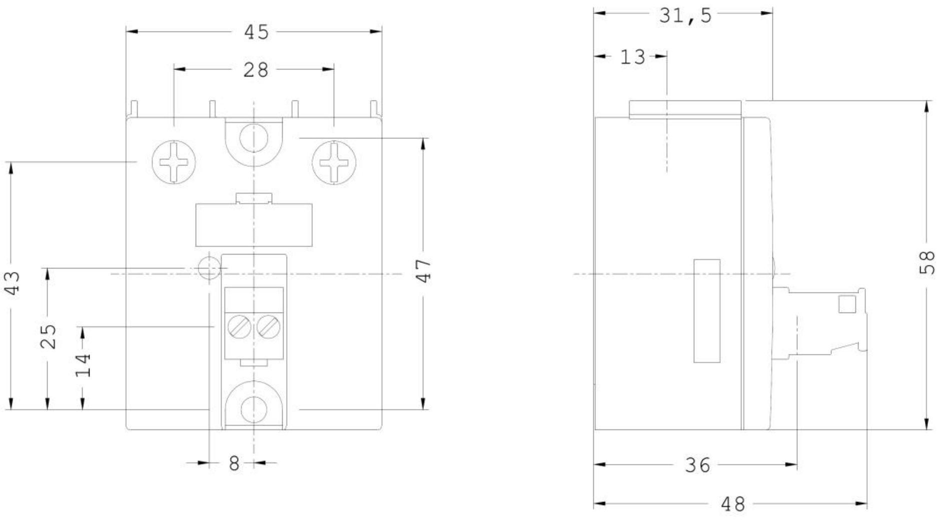

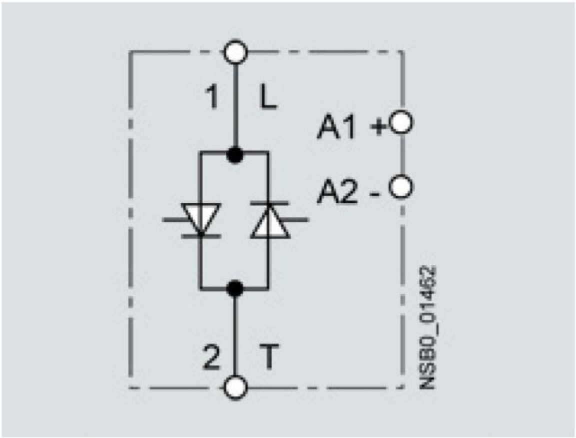

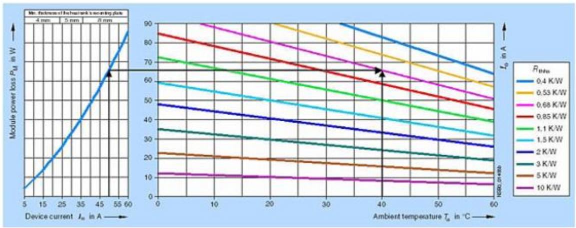

last change: Mar 4, 2013

Measuring equipment (WT230/WT210)

Basic Characteristics

Example of Frequency-power Accuracy Characteristics

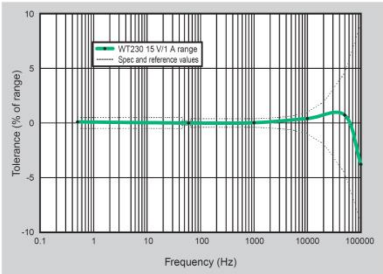

Example of WT210 Current Accuracy

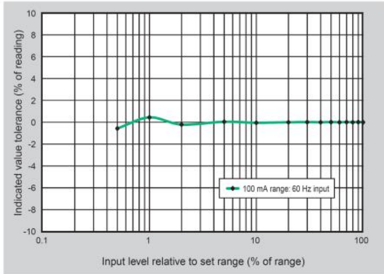

Current Input Surge Withstanding Ability

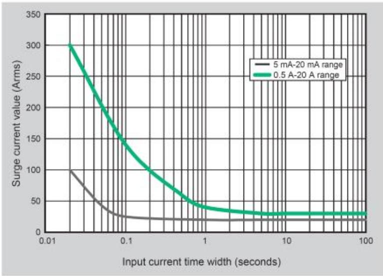

Example of Influence of Common Mode Voltage

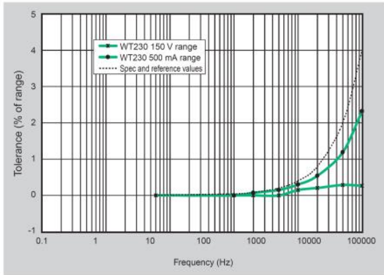

Example of D/A Output Response

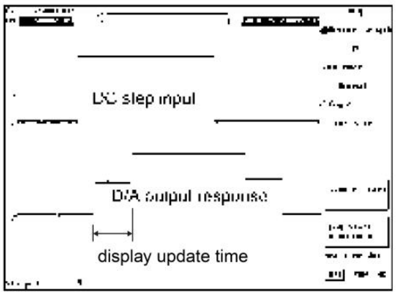

Comparison with Former Models

	WT200/WT130	WT210/WT230
Voltage input terminal	Binding post	Plug-in terminal (safety terminal)
External input terminal	Plug-in terminal (safety terminal)	BNC
Voltage and current basic accuracy	0.25% of rng	0.2% of rng
Power basic accuracy	0.3% of rng (WT200) 0.35% of rng (WT130)	0.2% of rng
Frequency range	DC, 10 Hz to 20 kHz	DC, 0.5 Hz to 100 kHz
Assured accuracy range	10% to 130% of range rating	1% to 130% of range rating
Display updating interval	0.25 second (fixed)	0.1/0.25/0.5/1/2/5 seconds
V, A, W display digits	4 digits (WT130) 5 digits (WT200)	5 digits
Line filter function	No	Yes (fc = 500 Hz)
Frequency filter function	Yes (fc = 300 Hz)	Yes (fc = 500 Hz)
Key lock	No	Yes
Harmonic measurement display updating interval	Approximately 3 seconds	0.25/0.5/1/2/5 seconds
Remote signals when comparator is installed	EXT HOLD and EXT TRIG are added. EXT START, EXT STOP, EXT RESET, and INTEG BUSY are not added.	All six signals listed to the left are added. Pin assign is changed.
Online data format	ASCII	ASCII, binary
Waveform data communications output	No	Yes (need /HRM)
Addressable mode B for GP-IB communications	Yes	No
Display digits (factory default)	4 digits	5 digits
Online output data digits (factory default)	4 digits	5 digits

Functions Included with the WT200 (but Not Included with the WT130) and Included with the WT210/WT230

- MAX hold function
- Moving decimal point display based on integrated power value
- 10,000-hour maximum integration time
- Integration with few data omissions
- Average active power display

WT230

WT210

Specifications

The latest product information is available at our web site http://www.yokogawa.com/tm/. Review the specifications to determine which model is right for you.

Input Specifications

Parameter	Voltage	Current
Input type	Floating input	
	Resistance voltage divider	Shunt input system
Rated values (ranges)	15/30/60/150/300/600 V	Direct input: 5/10/20/50/100/200 mA (WT210 only)[1] ; 0.5/1/2/5/10/20 A (WT210/WT230) External input (optional): 2.5/5/10 V or 50/100/200 mV
Measuring instrument loss (input resistance)	Input resistance: Approximately 2 MΩ Input capacitance: Approximately 13 pF	Direct input: Approximately 500 mΩ + approximately 0.1 µH (5-200 mA; WT210) Approximately 6 mΩ + 10 mΩ (max)[2] + approximately 0.1 µH (0.5-20 A; WT210) Approximately 6 mΩ approximately 0.1 µH (0.5-20 A; WT230) External input: Approximately 100 kΩ (2.5/5/10 V), approximately 20 kΩ (50/100/200 mV)
Maximum instantaneous allowed input (1 cycle, 20 ms duration)	Peak voltage of 2.8 kV or rms value of 2.0 kV (whichever is less)	0.5-20 A (WT210/WT230): Peak current of 450 A or rms value of 300 A (whichever is less) 5-200 mA (WT210): Peak current of 150 A or rms value of 100 A (whichever is less) External input: Peak value of 10 times range or less
Maximum instantaneous allowed input (1 second duration)	Peak voltage of 2.0 kV or rms value of 1.5 kV (whichever is less)	0.5-20 A (WT210/WT230): Peak current of 150 A or rms value of 40 A (whichever is less) 5-200 mA (WT210): Peak current of 30 A or rms value of 20 A (whichever is less) External input: Peak value of 10 times range or less
Maximum continuous allowed input	Peak voltage of 1.5 kV or rms value of 1.0 kV (whichever is less)	0.5-20 A (WT210/WT230): Peak current of 100 A or rms value of 30 A (whichever is less) 5-200 mA (WT210): Peak current of 30 A or rms value of 20 A (whichever is less) External input: Peak value of 5 times range or less
Maximum continuous common mode voltage (with 50/60 Hz input)	600 Vrms (with output connector protective cover), CAT II / 400 Vrms (without output connector protective cover) CAT II	
CMRR 600 Vrms across input terminal and case	50/60 Hz, -80 dB or higher (±0.01% of range or less) with voltage input terminals shorted and current input terminals open and external input terminals shorted Reference value (up to 100 kHz): ±((Maximum range rating)/(Range rating) × 0.001 × f% of rng) or less (voltage range and 0.5-20 A current range and external input range[3]) ±((Maximum range rating)/(Range rating) × 0.0002 × f% of rng) or less (WT210; 5-200 mA range) Note: 0.01% or higher. f is in kHz. 3 Decuple the above-formula about the external input range.	
Input terminal type	Plug-in terminal (safety terminal)	Direct input: Large binding post External input: BNC connector (insulation type)
A/D converter	Simultaneous conversion of voltage and current inputs Resolution: 16 bits Maximum conversion speed: Approximately 20 µs (approximately 51 kHz)	
Range switching	Ranges can be set manually, automatically, or through online controls. Auto-range function Range raising: When a measurement exceeds 130% of the rating, or when the peak value exceeds approximately 300% of the rating Range lowering: When a measurement falls to 30% or less of the rating, and the peak value falls to approximately 300% or less of the rating for the low range	
Measurement mode switching	Any of the following, selected manually or through online controls: RMS (true rms value measurements for both voltage and current), V MEAN (calibration of average-value-rectified rms value for voltage; true rms value measurement for current), DC (simple averages for both voltage and current)	

Note: Current direct input and external sensor input cannot both be used at the same time. When you operate current input terminals and external input terminals, please be careful.
Since these terminals are electrically connected inside the instrument.
1, Connect wires that match the size of the measurement current.
2, Factory setting

Measurement Functions

Parameter	Voltage/current	Active power
System	Digital sampling; sum of averages method	
Frequency range	DC, and 0.5 Hz to 100 kHz	
Crest factor	3 (with rated input) 300 (with minimum effective input)	
Accuracy (three months after calibration) (Conditions) Temperature: 23±5°C Humidity: 30-75% RH Input waveform: Sinewave Power factor: cosφ = 1 In-phase voltage: 0 V DC Frequency filter: ON at 200 Hz or less Scaling: OFF Display digits: 5 digits After CAL is executed Note: In the accuracy calculation formula, f is in kHz.	DC: ±(0.2% or rdg + 0.2% of rng)* 0.5 Hz ≤ f < 45 Hz: ±(0.1% of rdg + 0.2% of rng) 45 Hz ≤ f ≤ 66 Hz: ±(0.1% of rdg + 0.1% of rng) 66 Hz < f ≤ 1 kHz: ±(0.1% of rdg + 0.2% of rng) 1 kHz < f ≤ 10 kHz: ±((0.07 × f)% of rdg + 0.3% of rng) 10 kHz < f ≤ 100 kHz: ±((0.5% of rdg + 0.5% of rng) ±((0.04 × (f-10))% of rdg) * Add ±10 µA to the current DC accuracy.	DC: ±(0.3% or rdg + 0.2% of rng)* 0.5 Hz ≤ f < 45 Hz: ±(0.3% of rdg + 0.2% of rng) 45 Hz ≤ f ≤ 66 Hz: ±(0.1% of rdg + 0.1% of rng) 66 Hz < f ≤ 1 kHz: ±(0.2% of rdg + 0.2% of rng) 1 kHz < f ≤ 10 kHz: ±(0.1% of rdg + 0.3% of rng) ±((0.067 × (f-1))% of rdg) 10 kHz < f ≤ 100 kHz: ±(0.5% of rdg + 0.5% of rng) ±((0.09 × (f-10))% of rdg) * Add ±10 µA × voltage reading to the power DC accuracy.
Power factor effect Note: In the accuracy calculation formula, f is in kHz.	—	For cosφ = 0 45 Hz ≤ f ≤ 66 Hz: ±0.2% of VA (VA is a reading value of apparent power) Reference data (up to 100 kHz): ±((0.2 + 0.2 × f)% of VA) Indicated value tolerance for 0 < cosφ < 1 Add (tanφ × (effect when cosφ = 0)% of power reading to the above power accuracy. Note: φ is the phase angle between voltage and current.
Effective input range	1-130% of voltage/current range rating (for accuracy at 110-130%, add the reading tolerance × 0.5 to the above accuracy)	
Accuracy (12 months after calibration)	Add the accuracy's reading tolerance (three months after calibration) × 0.5 to the accuracy three months after calibration.	
Line filter function	A low-pass filter can be inserted in the input circuit for measurement. The cutoff frequency (fc) is 500 Hz.	
Accuracy with line filter on	Voltage and current: Add 0.2% of rdg at 45-66 Hz. Add 0.5% of rdg below 45 Hz. Power: Add 0.3% of rdg at 45-66 Hz. Add 1% of rdg below 45 Hz.	
Temperature coefficient	±0.03% of range/°C at 5-18°C and 28-40°C.	
Display updating intervals	0.1/0.25/0.5/1/2/5 seconds	
Lead/lag detecting	Lead/lag is detected correctly when phase difference equal to or greater than ±5° with both voltage and current inputs as sine waves equal to or greater than 50% of rated range-value, and the frequency is between 20 Hz to 2 kHz.	
Measurement lower limit frequency	Data updating rate: 0.1 second, 0.25 second, 0.5 second, 1 second, 2 seconds, 5 seconds Measurement lower limit frequency: 25 Hz, 10 Hz, 5 Hz, 2.5 Hz, 1.5 Hz, 0.5 Hz	

rng: Range rdg: Reading

Frequency Measurements

Measurement inputs: V1, V2, V3, A1, A2, or A3 (select one)
Measurement system: Reciprocal system
Measurement frequency ranges
100 ms: 25 Hz ≤ f ≤ 100 kHz
250 ms: 10 Hz ≤ f ≤ 100 kHz
500 ms: 5 Hz ≤ f ≤ 100 kHz
1 sec: 2.5 Hz ≤ f ≤ 100 kHz
2.5 sec: 1.5 Hz ≤ f ≤ 50 kHz
5 sec: 0.5 Hz ≤ f ≤ 20 kHz
Accuracy: ±(0.06% of rdg)
Conditions: Input equal to at least 30% of voltage/current rated range.
Frequency filter function ON at 200 Hz and below.
Frequency filter cutoff frequency: 500 Hz

Communication Functions (Optional for the WT210)

GP-IB or serial interface (RS-232-C) (select one)
GP-IB
Electrical and mechanical specifications:
Conform to IEEE Standard 488-1978 (JIS C1901-1987).
Functional specifications:
SH1, AH1, T5, L4, SR1, RL1, PR0, DC1, DT1, C0
Protocol: Conforms to IEEE Standard 488.2-1992.
Code used: ISO (ASCII) code
Addresses: 0-30 talker/listener addresses can be set.
Serial interface (RS-232-C)
Transmission mode: Asynchronous
Baud rates: 1200, 2400, 4800, 9600 bps

Specifications

Calculation Functions

		Single-phase 3-wire	Three-phase 3-wire (2 voltages, 2 currents)	Three-phase 3-wire (3 voltages, 3 currents)	Three-phase 4-wire
Voltage ΣV		(V1 + V3)/2		(V1 + V2 + V3)/3	
Current ΣA		(A1 + A3)/2		(A1 + A2 + A3)/3	
Active power ΣW		W1 + W3			W1 + W2 + W3
Reactive power var, Σvar	$var_i = \sqrt{(VA^2 - W^2)}$	var1 + var3			var1 + var2 + var3
Apparent power VA, ΣVA	VAi = Vi × Ai	VA1 + VA3	$\frac{\sqrt{3}}{2}$(VA1 + VA3)	$\frac{\sqrt{3}}{3}$(VA1 + VA2 + VA3)	VA1 + VA2 + VA3
Power factor PF, ΣPF	Pfi = Wi/VAi	ΣW/ΣVA			
Phase angle deg, Σdeg	degi = $\cos^{-1}$ (Wi/VAi)	$\cos^{-1}$ (ΣW/ΣVA)			

Notes

1. This equipment's apparent power (VA), reactive power (var), power factor (PF), and phase angle (deg) are calculated from voltage, current, and active power. (Therefore, if the input contains a distorted wave, the values may not match those of other measuring instruments based on different measurement principles.)
2. If either voltage or current falls to 0.5% of the range rating or less, then the apparent power (VA) and reactive power (var) are displayed as zero, and errors are displayed for power factor (PF) and phase angle (deg).
3. The sign of the var of each phase is displayed with +(positive). In the Σvar calculation, the var value for each phase is calculated with a negative sign if the current input leads the voltage input, and with a positive sign if the current input lags the voltage input. Then the value of Σ var may be displayed with –(negative).
4. Apparent power (VA) and reactive power (var) cannot be calculated and displayed at the harmonics measurement mode.

Display Functions

Display unit: 7-segment LED (light-emitting diode)
Display areas: 3

Display area	Displayed information
A	V, A, W, VA, var (for each element), integration elapsed time
B	V, A, W, PF, deg (for each element, percentage (content percentage, THD)
C	V, A, W, V/AHz, Vpk, Apk, ±Wh, ±Ah (for each element), MATH

Measurement parameters	Maximum display	Display resolution
V, A, W, VA, var	99999	0.001%
PF	±1.0000	0.01%
deg	±180.0	0.1°
±Wh, ±Ah	999999	0.0001%
VHz, AHz	99999	Input frequency/20,000

Display digits: 4 or 5 digits (selectable by user).
Factory default setting is 5 digits.

Units: m, k, M, V, A, W, VA, var, Hz, h±, deg, %
Display updating intervals: 0.1/0.25/0.5/1/2/5 seconds
Response time: Maximum 2 times the display updating interval (time required for display value to enter accuracy range of final value with line filter off, when range rating abruptly changes from 0% to 100%, and from 100% to 0%)
Maximum display: 140% of voltage/current range rating
Minimum display: About Vrms, Arms, and Ah, 0.5% of range rating. Less than 0.5% is zero suppression.
Display scaling function
Effective digits: Selected automatically according to the digits in the voltage and current ranges.
Setting range: 0.001 to 9999
Averaging function
There are two averaging methods (selectable by user):
Exponential average
Moving average
In cases where response can be set and exponential average is used, the attenuation constant can be selected. In cases where a moving average is used, the number of averages N can be selected from 8, 16, 32, and 64.
Auto-range monitor
An LED turns on when the input value is outside the range set for the auto-range.
MAX hold function
This function can be used to hold V, A, W, VA, var, Vpk, and Apk at maximum values.
MATH functions
System: When a function key on DISPLAY C is pressed to select the MATH functions, it is possible to perform efficiency (WT230 only) and input crest factor measurements, as well as arithmetic calculations on DISPLAY A and B measurements. In addition, it is possible to display average active power for time-converted integrated power.

Integration Functions

Display resolution: The minimum display resolution changes together with the integrated value.
Maximum display: -99999 to 999999 MWh/MAh
Modes: Standard integration mode (timer mode), continuous integration mode (repeat mode), manual integration mode
Timer: Automatic integration start/stop based on timer setting. Setting range: 000 h:00 min:00 sec to 10000 h:00 min:00 sec (If the time is set to zero, manual mode is automatically set.)
Count over flow: When the integrated value exceeds 999999 MWh/MAh or falls to at least -99999 MWh/MAh, the elapsed time is saved and the operation is stopped.
Accuracy: ±(display accuracy + 0.1% of rdg)
Timer accuracy: ±0.02%
Remote control: Starting, stopping, and resetting can be controlled through external contact signals. This function is only available when option /DA4, /DA12 or /CMP is installed.

Internal Memory Functions

Measurement data

Stored data	Normal measurement	Harmonic measurement
WT210 (760401)	Data for 600 samples	Data for 30 samples
WT230 (760502)	Data for 300 samples	Data for 30 samples
WT230 (760503)	Data for 200 samples	Data for 30 samples

Store interval: Display updating interval and 1 second to 99 hours, 59 minutes, and 59 seconds
Recall interval: Display updating interval and 1 second to 99 hours, 59 minutes, and 59 seconds
(Both can be set in 1-second increments.)
Panel setting information: Four different patterns of panel setting information can be written/read.

Harmonic Measurement Function (optional)

System: PLL synchronization
Measurement frequency range:
Fundamental frequency in range of 40-440 Hz
Maximum display: 99999
Display digits: 4 or 5 digits (selectable by user).
Factory default setting is 5 digits.
Measurement parameters: V, A, W, deg (WT210), V1, V2, V3, A1, A2, A3, W1, W2, W3, deg1, deg2, deg3 (WT230), individual harmonic levels, rms voltage, rms current, active power, fundamental frequency PF, harmonic distortion rate, individual harmonic content
Measurement element: These parameters can only be measured simultaneously for a single specified input element.

Sampling speed, window width, and analysis orders
The values for these parameters vary according to the input fundamental frequency as shown below.

Fundamental frequency	Sampling speed	Window width	Analysis orders
40 ≤ f < 70 Hz	f × 512 Hz	2 periods of f	50
70 ≤ f < 130 Hz	f × 256 Hz	4 periods of f	50
130 ≤ f < 250 Hz	f × 128 Hz	8 periods of f	50
250 ≤ f ≤ 440 Hz	f × 64 Hz	16 periods of f	30

FFT data length: 1024
FFT processed word length: 32 bits
Window function: Rectangular
Display updating interval:
0.25/0.5/1/2/5 seconds Updating is slower during online output according to the communication speed and the number of parameters transferred.
Accuracy: Add ±0.2% of range to normal measurement accuracy.
Note: For nth-order component input, add ((nth order reading) × (10/(m+1))%) to the n+mth order and n-mth order.

D/A Output (optional)

Output voltage: ±5 V FS (maximum approximately ±7.5 V) for each rated value
Number of outputs: 12 parameters with /DA12 option; 4 parameters with /DA4 option
Output data selection: Can be set separately for each channel.
Accuracy: ±(equipment accuracy + 0.2% of FS)
D/A converter: 12-bit resolution
Response time: Maximum 2 times the display updating interval
Updating interval: Same as the equipment's display updating interval
Temperature coefficient: ±0.05%/°C of FS
Output type

Frequency

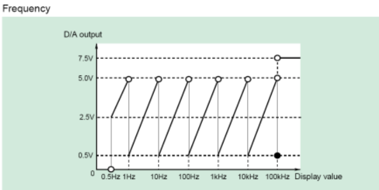

Integration

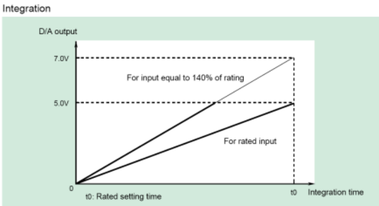

Other parameters

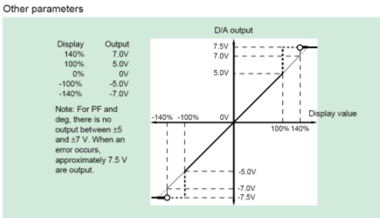

External Input (Optional)

Select either /EX1 or /EX2 for the voltage output-type current sensor.
/EX1: 2.5/5/10 V
/EX2: 50/100/200 mV
Specifications: See the section on input specifications.

Comparator Output (Optional)

Output method: Normal-open and normal-close relay contact output (pair)
Number of output parameters and settings:
Four parameters; can be set separately on each output channel.
Contact capacitance: 24 V/0.5 A
D/A output (4-channel): See section on D/A output (optional)

External Control Signal (with D/A or /CMP Option Only)

External control signals: EXT-HOLD, EXT-TRIG, EXT-START, EXT-STOP, EXT-RESET, INTEG-BUSY
Input: TTL level negative pulse

General Specifications

Warmup time: Approximately 30 minutes
Operating temperature and humidity ranges: 5-40˚C, 20-80% RH (no condensation)
Storage temperature: -25-60˚C (no condensation)
Maximum operating elevation: 2000 meters
Insulating resistance: 50 MΩ or higher at 500 V DC across all of the following areas:
Voltage input terminals (ganged) and case
Current input terminals (ganged) and case
Voltage input terminals (ganged) and current input terminals (ganged)
Voltage input terminals (ganged) of each element
Current input terminals (ganged) of each element
Voltage input terminals (ganged) and power plug
Current input terminals (ganged) and power plug
Case and power plug
Insulating withstand voltage:
3700 V for one minute at 50/60 Hz across all of the following areas:
Voltage input terminals (ganged) and case
Current input terminals (ganged) and case
Voltage input terminals (ganged) and current input terminals (ganged)
Voltage input terminals (ganged) of each element
Current input terminals (ganged) of each element
Voltage input terminals (ganged) and power plug
Current input terminals (ganged) and power plug
1500 V for one minute at 50/60 Hz across case and power plug

Power supply: Free power supply (100-240 V), 50/60 Hz frequency
Consumed power: Max 35 VA for WT210, max 55 VA for WT230
External dimensions for WT210:
Approximately 213 × 88 × 379 mm (WHD) (excluding projections)
External dimensions for WT230:
Approximately 213 × 132 × 379 mm (WHD) (excluding projections)
Weight: Approximately 3 kg for WT210, approximately 5 kg for WT230
Safety standard Complying standard EN61010-1
Overvoltage category (Installation category) II
Pollution degree 2
Emission Complying standard EN61326 Class A
EN61000-3-2
EN61000-3-3
AS/NZS 2064 Class A
Immunity Complying standard EN61326 Annex A

■ Exterior View

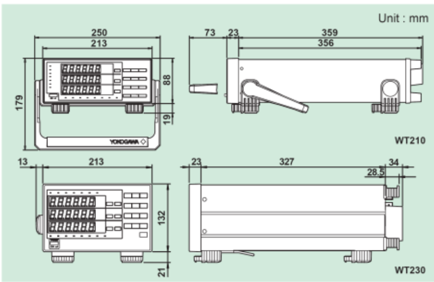

■ Model Numbers and Suffix Codes

Model number	Suffix code	Description	
760401		WT210 single-input element model	
Power cord	-D	UL/CSA standard	
	-F	VDE standard	
	-R	AS standard	
	-Q	BS standard	
Options	/C1	GP-IB communication interface	Select one
	/C2	Serial (RS-232-C) communication interface	
	/EX1	External input 2.5/5/10 V	Select one
	/EX2	External input 50/100/200 mV	
	/HRM	Harmonic measurement function	
	/DA4	4-channel DA output	Select one
	/CMP	Comparator and D/A, 4 channels each	

Note: The WT210 communication interface cannot be changed or modified after delivery.

Model number	Suffix code	Description	
760502		WT230 2-input element model	
760503		WT230 3-input element model	
Interface	-C1	GP-IB communication interface	Select one
	-C2	Serial (RS-232-C) communication interface	
Power cord	-D	UL/CSA standard	
	-F	VDE standard	
	-R	AS standard	
	-Q	BS standard	
Options	/EX1	External input 2.5/5/10 V	
	/EX2	External input 50/100/200 mV	Select one
	/HRM	Harmonic measurement function	
	/DA12	12-channel DA output	
	/CMP	Comparator and D/A, 4 channels each	Select one

■ Standard Accessories

Power cord, Power fuse, Current input protective cover, Rubber feet for the hind feet, 24-pin connector (provided only on options/DA4, /DA12, and /CMP), User's manual

■ Wiring Types and Model Numbers

Wiring / Model	760401	760502	760503
Single-phase 2-wire	✓	✓	✓
Single-phase 3-wire	–	✓	✓
Three-phase 3-wire (2 voltages, 2 currents)	–	✓	✓
Three-phase 3-wire (3 voltages, 3 currents)	–	–	✓
Three-phase 4-wire	–	–	✓

■ Rack mounts

Product	Model or part number	Specification	Order quantity
Rack mounting kit	751533-E2	For WT210 EIA standalone installation	1
Rack mounting kit	751533-J2	For WT210 JIS standalone installation	1
Rack mounting kit	751534-E2	For WT210 EIA connected installation	1
Rack mounting kit	751534-J2	For WT210 JIS connected installation	1
Rack mounting kit	751533-E3	For WT230 EIA standalone installation	1
Rack mounting kit	751533-J3	For WT230 JIS standalone installation	1
Rack mounting kit	751534-E3	For WT230 EIA connected installation	1
Rack mounting kit	751534-J3	For WT230 JIS connected installation	1

Ask Yokogawa for information on rack mounts in which WT210 and WT230 are combined.

■ Accessories (sold separately)

Model number	Description	
B9317WD	1.5 mm hex wrench	For fastening cable on 758931
B9284LK	External sensor cable	For external input; 50 cm